eLife

Reviewed Preprint
v2 • June 28, 2024
Revised by authors

Reviewed Preprint
v1 • January 17, 2024

Neuroscience

The Spatial Frequency Representation Predicts Category Coding in the Inferior Temporal Cortex

Ramin Toosi, Behnam Karami, Roxana Koushki, Farideh Shakerian, Jalaledin Noroozi, Ehsan Rezayat, Abdol-Hossein Vahabie, Mohammad Ali Akhaee, Mohammad-Reza A. Dehaqani

School of Electrical and Computer Engineering, College of Engineering, University of Tehran, Tehran, Iran • Cognitive Systems Laboratory, Control and Intelligent Processing Center of Excellence (CIPCE), School of Electrical and Computer Engineering, College of Engineering, University of Tehran, Tehran, Iran • School of Cognitive Sciences, Institute for Research in Fundamental Sciences (IPM), Tehran, Iran • Perception and Plasticity Group, German Primate Center, Leibniz Institute for Primate Research, 37077 Gottingen, Germany • Neural Circuits and Cognition Lab, European Neuroscience Institute Gottingen - A Joint Initiative of the University Medical Center Gottingen and the Max Planck Society, 37077 Gottingen, Germany • Department of Brain and Cognitive Sciences, Cell Science Research Center, Royan Institute for Stem Cell Biology and Technology, ACECR, Tehran, Iran • Department of Physiology, Faculty of Medical Sciences, Tarbiat Modares University, Tehran, Iran • Department of Psychology, Psychology and Educational Science Faculty, University of Tehran, Tehran, Iran

Abstract

Understanding the neural representation of spatial frequency (SF) in the primate cortex is vital for unraveling visual processing mechanisms in object recognition. While numerous studies concentrate on the representation of SF in the primary visual cortex, the characteristics of SF representation and its interaction with category representation remain inadequately understood. To explore SF representation in the inferior temporal (IT) cortex of macaque monkeys, we conducted extracellular recordings with complex stimuli systematically filtered by SF. Our findings disclose an explicit SF coding at single-neuron and population levels in the IT cortex. Moreover, the coding of SF content exhibits a coarse-to-fine pattern, declining as the SF increases. Temporal dynamics analysis of SF representation reveals that low SF (LSF) is decoded faster than high SF (HSF), and the SF preference dynamically shifts from LSF to HSF over time. Additionally, the SF representation for each neuron forms a profile that predicts category selectivity at the population level. IT neurons can be clustered into four groups based on SF preference, each exhibiting different category coding behaviors. Particularly, HSF-preferred neurons demonstrate the highest category decoding performance for face stimuli. Despite the existing connection between SF and category coding, we have identified uncorrelated representations of SF and category. In contrast to the category coding, SF is more sparse and places greater reliance on the representations of individual neurons. Comparing SF representation in the IT cortex to deep neural networks, we observed no relationship between SF representation and category coding. However, SF coding, as a category-orthogonal property, is evident across various ventral stream models. These results dissociate the separate representations of SF and object category, underscoring the pivotal role of SF in object recognition.

eLife assessment

This **useful** study aimed to examine the relationship of spatial frequency selectivity of single macaque inferotemporal (IT) neurons to category selectivity. There are some interesting findings in this report but some of these findings were difficult to evaluate because several critical details of the analysis are **incomplete**. The conclusion that single-unit spatial frequency selectivity can predict object coding needs further evidence to confirm.

https://doi.org/10.7554/eLife.93589.2.sa2

Introduction

Spatial frequency (SF) constitutes a pivotal component of visual stimuli encoding in the primate visual system, encompassing the number of grating cycles within a specific visual angle. Higher SF (HSF) corresponds to intricate details, while lower SF (LSF) captures broader information. Previous psychophysical studies have compellingly demonstrated the profound influence of SF manipulation on object recognition and categorization processes (Joubert et al., 2007; Schyns and Oliva, 1994; Craddock et al., 2013; Caplette et al., 2014; Cheung and Bar, 2014; Ashtiani et al., 2017). Saneyoshi and Michimata (2015) and Jahfari (2013) have highlighted the significance of HSF and LSF for categorical/coordinate processing and in object recognition and decision making, respectively. The sequence in which SF content is presented also affects the categorization performance, with coarse-to-fine presentation leading to faster categorizations (Kauffmann et al., 2015). Considering face as a particular object, several studies showed that middle and higher SFs are more critical for face recognition (Costen et al., 1996; Hayes et al., 1986; Fiorentini et al., 1983; Cheung et al., 2008). Another vital theory suggested by psychophysical studies is the coarse-to-fine perception of visual stimuli, which states that LSF or global contents are processed faster than HSF or local contents (Schyns and Oliva, 1994; Rotshtein et al., 2010; Gao, 2011; Yardley et al., 2012; Kauffmann et al., 2015; Rokszin, 2016). Despite the extensive reliance on psychophysical studies to examine the influence of SF on categorization tasks, our understanding of SF representation within primate visual systems, particularly in higher visual areas like the inferior temporal (IT) cortex, remains constrained due to the limited research in this specific domain.

One of the seminal studies investigating the neural correlates of SF processing and its significance in object recognition was conducted by Bar (2003). Their research proposes a top-down mechanism driven by the rapid processing of LSF content, facilitating object recognition (Bar, 2003; Fenske et al., 2006). The exploration of SF representation has revealed the engagement of distinct brain regions in processing various SF contents (Fintzi and Mahon, 2014; Chaumon et al., 2014; Bermudez et al., 2009; Iidaka et al., 2004; Peyrin et al., 2010; Gaska et al., 1988; Bastin et al., 2013; Oram and Perrett, 1994). More specifically, the orbitofrontal cortex (OFC) has been identified as accessing global (LSF) and local (identity; HSF) information in the right and left hemispheres, respectively (Fintzi and Mahon, 2014). The V3A area exhibits low-pass tuning curves (Gaska et al., 1988), while HSF processing activates the left fusiform gyrus (Iidaka et al., 2004). Neural responses in the IT cortex, which play a pivotal role in object recognition and face perception, demonstrate correlations with the SF components of complex stimuli (Bermudez et al., 2009). Despite the acknowledged importance of SF as a critical characteristic influencing object recognition, a more comprehensive understanding of its

representation is warranted. By unraveling the neural mechanisms underlying SF representation in the IT cortex, we can enrich our comprehension of the processing and categorization of visual information.

To address this issue, we investigate the SF representation in the IT cortex of two passive-viewing macaque monkeys. We studied the neural responses of the IT cortex to intact, SF-filtered (five ranges), and phase-scrambled stimuli. SF decoding is observed in both population- and single-level representations. Investigating the decoding pattern of individual SF bands reveals a course-to-fine manner in recall performance where LSF is decoded more accurately than HSF. Temporal dynamics analysis shows that SF coding exhibits a coarse-to-fine pattern, emphasizing faster processing of lower frequencies. Moreover, SF representation forms an average LSF-preferred tuning across neuron responses at 70ms to 170ms after stimulus onset. Then, the average preferred SF shifts monotonically to HSF in time after the early phase of the response, with its peak at 220ms after the stimulus onset. The LSF-preferred tuning turns into an HSF-preferred one in the late neuron response phase.

Next, we examined the relationship between SF and category coding. We found a strong positive correlation between SF and category coding performances in sub-populations of neurons. SF coding capability of individual neurons is highly correlated with the category coding capacity of the sub-population. Moreover, clustering neurons based on their SF responses indicates a relationship between SF representation and category coding. Employing the neuron responses to five SF ranges considering only the scrambled stimuli, an SF profile was identified for each neuron that predicts the categorization performance of that neuron in a population of the neurons sharing the same profile. Neurons whose response increases with increasing SF encode faces better than other neuron populations with other profiles.

Given the co-existence of SF and category coding within the IT cortex and the prediction capability of SF for category selectively, we examined the neural mechanisms underlying SF and category representation. In single-level, we found no correlation between SF and category coding capability of single neurons. At the population level, we found that the contribution of neurons to SF coding did not correlate with their contribution to category coding. Delving into the characteristics of SF coding, we found that individual neurons carry more independent SF-related information compared to the encoding of categories (face vs. non-face). Analyzing the temporal dynamics of each neuron's contribution to population-level SF coding reveals a shift in sparsity during different phases of the response. In the early phase (70ms-170ms), the contribution is more sparse than category coding. However, this behavior is reversed in the late phase (170ms-270ms), with SF coding showing a less sparse contribution.

Finally, we compared the representation of SF in the IT cortex with several popular convolutional neural networks (CNNs). We found that CNNs exhibited robust SF coding capabilities with significantly higher accuracies than the IT cortex. Like the IT cortex, LSF content showed higher decoding performance than the HSF content. However, while there were similarities in SF representation, CNNs did not replicate the SF-based profiles predicting neuron category selectivity observed in the IT cortex. We posit that our findings establish neural correlates pertinent to behavioral investigations into SF's role in object recognition. Additionally, our results shed light on how the IT cortex represents and utilizes SF during the object recognition process.

Results

SF coding in the IT cortex

To study the SF representation in the IT cortex, we designed a passive stimulus presentation task (**Figure 1a**, see Materials and methods). The task comprises two phases: the selectivity and the main. During the selectivity phase, 155 stimuli, organized into two super-ordinate and four ordinate categories, were presented (with a 50ms stimulus presentation followed by a 500ms blank period, see Materials and methods). Next, the six most responsive stimuli are selected along with nine fixed stimuli (six faces and three non-face objects, **Figure 1b**) to be presented during the main phase (33ms stimulus presentation followed by a 465ms blank, see Materials and methods). Each stimulus is phase scrambled, and then the intact and scrambled versions are filtered in five SF ranges (R1 to R5, with R5 representing the highest frequency band, **Figure 1b**), resulting in a total of 180 unique stimuli presented in each session (see Materials and methods). Each session consists of 15 blocks, with each stimulus presented once per block in a random order. The IT neurons of passive viewing monkeys are recorded where the cells cover all areas of the IT area uniformly (**Figure 1a**). We only considered the responsive neurons (see Materials and methods), totaling 266 (157 M1 and 109 M2). A sample neuron (neuron #155, M1) peristimulus time histogram (PSTH) is illustrated in **Figure 1c** in response to the scrambled stimuli for R1, R3, and R5. R1 exhibits the most pronounced firing rate, indicating the highest neural activity level. In contrast, R5 displays the lowest firing rate, suggesting an LSF-preferred trend in the neuron's response. To explore the SF representation and coding capability of IT neurons, each stimulus in each session block is represented by an N element vector where the i'th element is the average response of the i'th neuron to that stimulus within a 50ms time window (see Materials and methods).

To assess whether individual neurons encode SF-related information, we utilized the linear discriminant analysis (LDA) method to predict the SF range of the scrambled stimuli based on neuron responses (see Materials and methods). **Figure 1d** displays the average time course of SF discrimination accuracy across neurons. The accuracy value is normalized by subtracting the chance level (0.2). At single-level, the accuracy surpasses the chance level by an average of 4.02% at 120 ms after stimulus onset. We only considered neurons demonstrating at least three consecutive time windows with accuracy significantly greater than the chance level, resulting in a subset of 105 neurons. The maximum accuracy of a single neuron was 19.08% higher than the chance level (unnormalized accuracy is 39.08%, neuron #193, M2). Subsequently, the SF decoding performance of the IT population is investigated (R1 to R5 and scrambled stimuli only, see Materials and methods). **Figure 1d** also illustrates the SF classification accuracy across time in population-level representations. The peak accuracy is 24.68% higher than the chance level at 115ms after the stimulus onset. These observations indicate the explicit presence of SF coding in the IT cortex. The strength of SF selectivity, considering the trial-to-trial variability is provided in **Appendix 1 - Figure 1**, by ranking the SF bands for each neuron based on half of the trials and then plotting the average responses for the obtained ranks for the other half of the trials. To determine the discrimination of each SF range, **Figure 1e** shows the recall of each SF content for the time window of 70ms to 170ms after stimulus onset. This observation reveals an LSF-preferred decoding behavior across the IT population (recall, R1=0.47±0.04, R2=0.36±0.03, R3=0.30±0.03, R4=0.32±0.04, R5=0.30±0.03, and R1 > R5, p-value<0.001).

Temporal dynamics of SF representation

The sample neuron and recall values in **Figure 1** indicate an LSF-preferred neuron response. To explore this behavior over time, we analyzed the temporal dynamics of SF representation. **Figure 2a** illustrates the onset of SF recalls, revealing a coarse-to-fine trend where R1 is decoded faster than R5 (onset times in milliseconds after stimulus onset, R1=84.5±3.02, R2=86.0±4.4, R3=88.9±4.9, R4=86.5±4.1, R5=97.15±4.9, R1 < R5, p-value<0.001). **Figure 2b** illustrates the time course of the average preferred SF across the neurons. To calculate the preferred SF for each neuron, we multiplied the firing rate by the SF range and normalized the values (see Materials and methods).

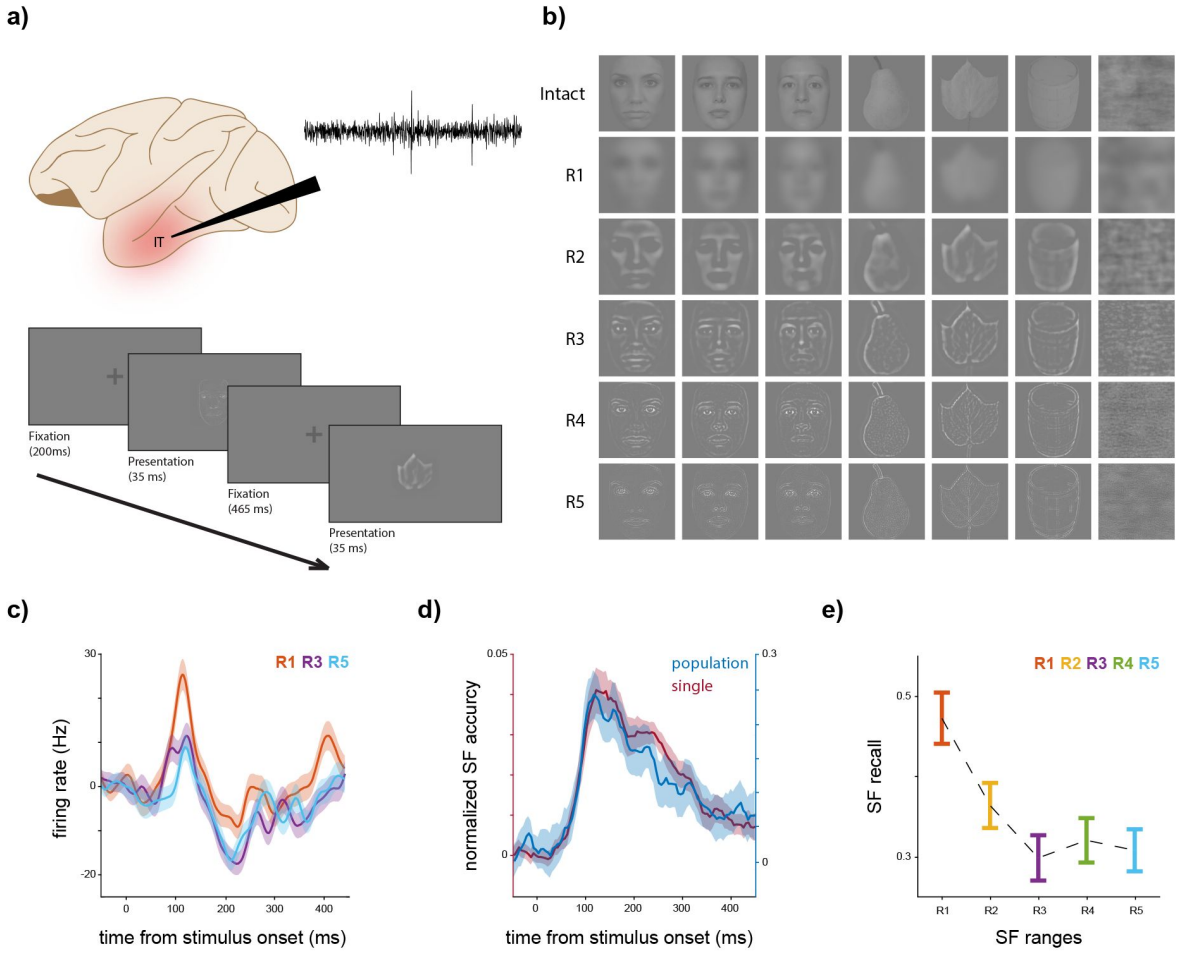

Figure 1.

Experimental design and SF coding.

a *Experimental design*. The design of the experiment involved the collection of responses from IT neurons to 15 stimuli (including six faces, three non-faces, and six selective stimuli, see Materials and methods) in six SF bands (intact and R1 to R5, see Materials and methods), and two versions (scrambled and unscrambled) using a passive presentation task. Presentation of blocks starts if the monkey preserves fixation for 200ms. Each block consisted of a 33ms stimulus presentation followed by a blank screen with a fixation point of 465ms, and each stimulus was presented 15 times. The recorded signals were sorted, and visually responsive neurons were selected (N = 266, see Materials and methods). **b** *A sample of the fixed stimulus set*. This panel shows three (out of six) faces, three non-faces, and one scrambled sample stimulus. Each row corresponds to an SF range starting with intact, followed by R1 to R5 (low to high SF). **c** *A sample neuron*. The PSTH of a sample neuron (N = 151, M1) for scrambled stimuli is depicted. To generate a response vector for a given stimulus or trial, the responses of each neuron were averaged in a 50ms time window centered around the relevant time point. The PSTH was smoothed using a Gaussian kernel with a standard deviation of 20ms. The responses of three SF bands (R1, R3, and R5) are shown for better illustration. **d** *SF coding exists in the IT cortex*. The decoding performance of SF ranges using scrambled stimuli is shown over time. Single-level and population-level representations were fed into an LDA algorithm to predict the SF range of the scrambled stimuli. Shadows illustrate the SEM and STD for single and population levels, respectively. This figure highlights the presence of SF coding in both individual and population neural activity. **e** *LSF-preferred nature of SF coding*. The population recall of each SF band in response to scrambled stimuli, determined using the LDA method, is presented. The error bars indicate the STD. The results demonstrate a decreasing trend as SF moves towards higher frequencies, suggesting a coarse-to-fine decoding preference.

Figure 2b demonstrates that following the early phase of the response (70ms to 170ms), the average preferred SF shifts towards HSF, reaching its peak at 215ms after stimulus onset (preferred SF, 0.54±0.15). Furthermore, a second peak emerges at 320 ms after stimulus onset (preferred SF, 0.22±0.16), indicating a shift in the average preferred SF in the IT cortex towards higher frequencies. To analyze this shift, we divided the time course into two intervals of 70ms to 170ms, where the response peak of the neurons happens, and 170ms to 270ms, where the first peak of SF preference occurs. We calculated the percentage of the neurons that significantly responded to a specific SF range higher than others (one-way ANOVA with a significance level of 0.05, see Materials and methods) for the two time intervals. **Figure 2c** and **d** show the percentage of the neurons in each SF range for the two time steps. In the early phase of the response (T1, 70ms to 170ms), the highest percentage of the neurons belong to R1, 40.19%, and a decreasing trend is observed as we move towards higher frequencies (R1=40.19%, R2=19.60%, R3=13.72%, R4=10.78%, R5=15.68%). Moving to T2, the percentage of neurons responding to R1 higher than the others remains stable, dropping to 38.46%. The number of neurons in R2 also drops to under 5% from 19.60% observed in T1. On the other hand, the percentage of the neurons in R5 reaches 46.66% in T2 compared to 15.68% in T1 (higher than R1 in T1). This observation indicates that the increase in preferred SF is due to a substantial increase in the selective neurons to HSF, while the response of the neurons to R1 is roughly unchanged. To further understand the population response to various SF ranges, the average response across neurons for R1 to R5 is depicted in **Figure 2c** and **d** (bottom panels). In the first interval, T1, an average LSF-preferred tuning is observed where the average neuron response decreases as the SF increases (normalized firing rate for R1=1.09±0.01, R2=1.05±0.01, R3=1.03±0.01, R4=1.03±0.02, R5=1.00±0.01, Bonferroni corrected p-value for R2<R5, 0.006). Considering the strength of responses to scrambled stimuli, the average firing rate in response to scrambled stimuli is 26.3 Hz, which is significantly higher than the response observed between -50 and 50 ms, where it is 23.4 Hz (p-value=3×10^{-5}). In comparison, the mean response to intact face stimuli is 30.5 Hz, while non-face stimuli elicit an average response of 28.8 Hz. The distribution of neuron responses for scrambled, face, and non-face in T1 is illustrated in **Appendix 1 - Figure 2**. During the second time interval, excluding R1, the decreasing pattern transformed to an increasing one, with the response to R5 surpassing that of R1 (normalized firing rate for R1=0.80±0.02, R2=0.73±0.02, R3=0.76±0.02, R4=0.81±0.02, R5=0.84±0.01, Bonferroni corrected p-value for R2<R4, 0.022, R2<R5, 0.0003, and R3<R5, 0.03). Moreover, the average firing rates of scrambled, face, and non-face stimuli are 19.5 Hz, 19.4 Hz, and 22.4 Hz, respectively. The distribution of neuron responses is illustrated in **Appendix 1 - Figure 2**. These observations illustrate an LSF-preferred tuning in the early phase of the response, shifting towards HSF-preferred tuning in the late response phase.

SF profile predicts category coding

Our findings indicate explicit SF coding in the IT cortex. Given the co-existence of SF and category coding in this region, we examine the relationship between SF and category codings. As depicted in **Figure 2**, while the average preferred SF across the neurons shifts to HSF, the most responsive SF range varies across individual neurons. To investigate the relation between SF representation and category coding, we identified an SF profile by fitting a quadratic curve to the neuron responses across SF ranges (R1 to R5, phase-scrambled stimuli only). Then, according to the fitted curve, an SF profile is determined for each neuron (see Materials and methods). Five distinct profiles were identified based on the tuning curves (**Figure 3a**): i) flat, where the neuron has no preferred SF (not included in the results), ii) LSF preferred (LP), where the neuron response decreases as SF increases, iii) HSF preferred (HP), where neuron response increases as the SF shifts towards higher SFs, iv) U-shaped where the neuron response to middle SF is lower than that of HSF or LSF, and v) inverse U-shaped (IU), where the neuron response to middle SF is higher than that of LSF and HSF. The U-shaped and HSF-preferred profiles represent the largest and smallest populations, respectively. To check the robustness of the profiles, considering the trial-to-trial variability, the strength of SF selectivity in each profile is provided in **Appendix 1 - Figure 3**, by forming the profile of each neuron based on half of the trials and then plotting the

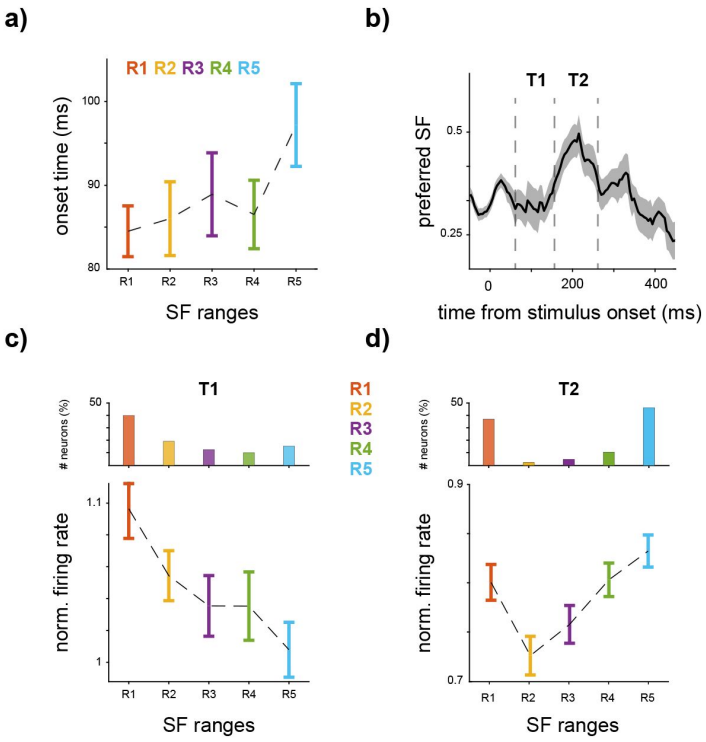

Figure 2.

The temporal dynamics of SF representation.

a *Course-to-fine nature of SF coding*. The onset time of the recall of each SF range in scrambled stimuli is illustrated, with error bars indicating the STD. The results suggest that the onset time of decoding increases as SF increases. **b** *SF preference shifts toward higher frequencies over time*. The time course of the average preferred SF (see Materials and methods) across neurons is illustrated. The average preferred SF of IT neurons moves towards higher frequencies from 170ms after stimulus onset, reaching its highest value at 220ms. A second peak emerges at 320ms following the stimulus onset. The SF preference shows a monotonic increase followed by a decrease in time. **c**,**d** *Shift in neural response towards HSF*. The average response of all neurons within the two time intervals (T1 and T2 in panel b) is shown, with error bars indicating the SEM. **c** In T1, from 70ms to 170ms after stimulus onset, a decreasing response of the neurons is observed as the SF content shifts towards higher frequencies. The relative percentage of neurons showing stronger responses to SF ranges (R1 to R5) in T1 is depicted in the inner top panel. R1 is the most responsive SF for roughly 40% of the neurons. **d** In the following interval (T2, 170ms to 270ms), an increasing tuning is observed from R2 to R5, where R5 elicits the highest firing rates. Furthermore, in T2, there is a roughly threefold increase in the percentage of neurons exhibiting stronger responses to R5 compared to T1, indicating a shift in the neurons' responses towards HSF (top panel).

average SF responses with the other half. Following profile identification, the object coding capability of each profile population is assessed. Here, instead of LDA, we employ the separability index (SI) introduced by Dehaqani et al. (2016), because of the LDA limitation in fully capturing the information differences between groups as it categorizes samples as correctly classified or misclassified.

To examine the face and non-face information separately, SI is calculated for face vs. scrambled and non-face vs. scrambled. **Figure 3a** displays the identified profiles and **Figure 3b** indicates the average SI value during 70ms to 170ms after the stimulus onset. The HSF preferred profile shows significantly higher face information compared to other profiles (face SI for LP=0.58±0.03, HP=0.89±0.05, U=0.07±0.01, IU=0.07±0.01, HP > LP, U, IU with p-value < 0.001) and than non-face information in all other profiles (non-face SI for LP=0.04±0.01, HP=0.02±0.01, U=0.19±0.03, IU=0.08±0.02, and face SI in HP is greater than non-face SI in all profiles with p-value < 0.001). This observation underscores the importance of middle and higher frequencies for face representation. The LSF-preferred profile also exhibits significantly higher face SI than non-face objects (p-value<0.001). On the other hand, in the IU profile, non-face information surpasses face SI (p-value<0.001), indicating the importance of middle frequency for the non-face objects. Finally, in the U profile, there is no significant difference between the face and non-face objects (face vs. non-face p-value=0.36).

To assess whether the SF profiles distinguish category selectivity or merely evaluate the neuron's responsiveness, we quantified the number of face/non-face selective neurons in the 70-170ms time window. Our analysis shows a total of 43 face-selective neurons and 36 non-face-selective neurons (FDR-corrected p-value < 0.05). The results indicate a higher proportion of face-selective neurons in LP and HP, while a greater number of non-face-selective neurons is observed in the IU category (number of face/non-face selective neurons: LP=13/3, HP=6/2, IU=3/9). The U category exhibits a roughly equal distribution of face and non-face-selective neurons (U=14/13). This finding reinforces the connection between category selectivity and the identified profiles. We then analyzed the average neuron response to faces and non-faces within each profile. The difference between the firing rates for faces and non-faces in none of the profiles is significant (face/non-face average firing rate (Hz): LP=36.72/28.77, HP=28.55/25.52, IU=21.55/27.25, U=38.48/36.28, Ranksum with significance level of 0.05). Although the observed differences are not statistically significant, they provide support for the association between profiles and categories rather than mere responsiveness.

Next, to examine the relation between the SF (category) coding capacity of the single neurons and the category (SF) coding capability of the population level, we calculated the correlation between coding performance at the population level and the coding performance of single neurons within that population (\figure name \ref{fig:profile}c and d). In other words, we investigated the relation between single and population levels of coding capabilities between SF and category. The SF (or category) coding performance of a sub-population of 20 neurons that have roughly the same single-level coding capability of the category (or SF) is examined. Neurons were sorted based on their SF or category performances, resulting in two separate groups of ranks—one for SF and another for category. Subsequently, we selected sub-populations of neurons with similar ranks according to SF or category (see Materials and methods). Each sub-population comprises 20 neurons with approximately similar SF (or category) performance levels. Then, the SF and category decoding accuracy is calculated for each sub-population. The scatterplot of individual vs. sub-population accuracy demonstrated a significant positive correlation between the sub-population performance and the accuracy of individual neurons within those populations. Specifically, the correlation value for SF-sorted and category-sorted groups is 0.66 (p-value=10^{-31}) and 0.39 (p-value=10^{-10}), respectively. This observation illustrates that SF coding capacity at single-level representations significantly predicts category coding capacity at the population level.

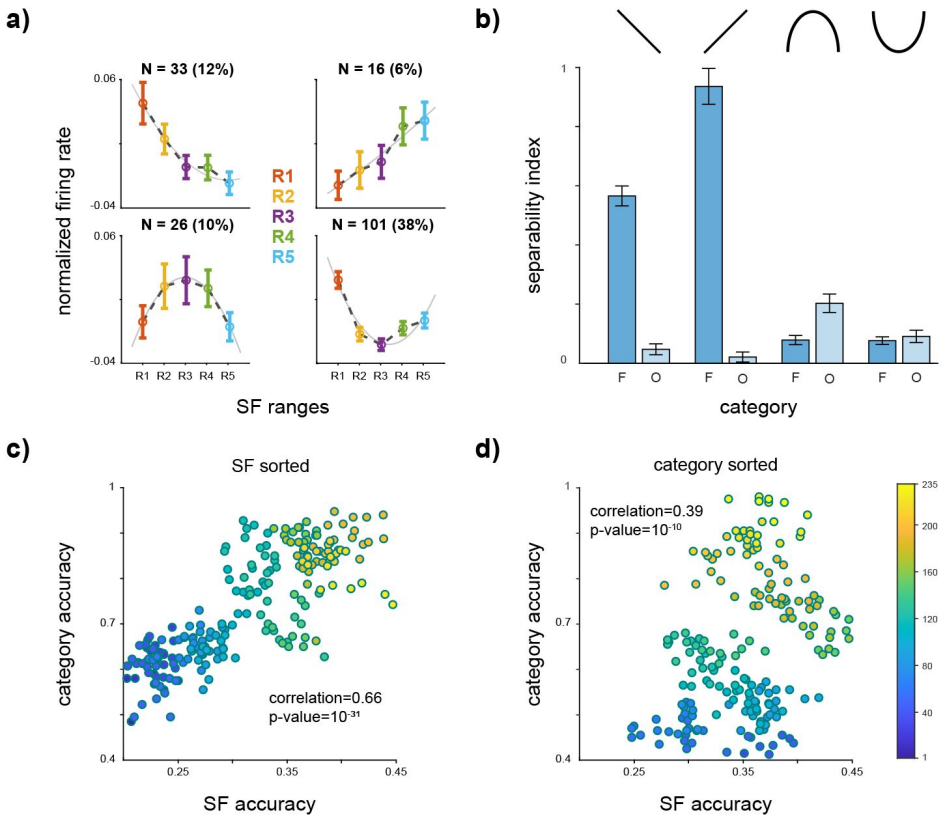

Figure 3.

SF profile predicts category coding.

a,**b** *SF proile predicts category selectivity*. **a** The responses of each neuron were standardized by subtracting the mean and dividing by the standard deviation of the baseline time. Neurons were then categorized into four groups based on the fitting of a quadratic function to their responses (see Materials and methods). Each panel presents the average neuron responses within each category for SF ranges R1 to R5, with error bars indicating the SEM of the response values. The percentage of the neurons in each category is displayed at the top of each panel. The "flat" category, where the response to no SF was higher than others, was excluded from this analysis. **b** SI of face/non-face vs. scrambled stimuli is illustrated (see Materials and methods). The SI value and SF profile are determined within the time window of 70ms to 170ms after stimulus onset. The HSF-preferred population exhibited significantly higher face SI compared to the other groups. The LSF-preferred population displayed a significant difference in face and non-face SI. On the other hand, the IU profile indicates a significantly higher SI value for the non-face compared to the face. The U-shaped profile did not show any significant differences between the face and the non-face. These results suggest that the neuron's response to various SF bands can predict its decoding capability. **c**,**d** *The relation between SF and category coding in sub-populations*. Initially, the LDA method was employed to calculate the individual neuron's performance in the single-level category and SF coding. Next, a sorting procedure based on SF (panel c) and category (panel d) coding performances were conducted to create sub-populations of neurons exhibiting similar capabilities (see Materials and methods). The scatter plot of the category and SF coding accuracy of these sub-populations demonstrated a notably high degree of positive correlation between SF and category accuracies in the IT cortex.

Uncorrelated mechanisms for SF and category coding

As both SF and category coding exist in the IT cortex at both the single neuron and population levels, we investigated their underlying coding mechanisms (for single level and population level separately). **Figure 4a** displays the scatter plot of SF and category coding capacity for individual neurons. The correlation between SF and category accuracy across individual neurons shows no significant relationship (correlation: 0.024 and p-value: 0.53), suggesting two uncorrelated mechanisms for SF and category coding. To explore the population-level coding, we considered neuron weights in the LDA classifier as indicators of each neuron's contribution to population coding. **Figure 4b** indicates the scatter plot of the neuron's weights in SF and category decoding. The LDA weights reveal no correlation between the patterns of neuron contribution in population decoding of SF and category (correlation=0.002 and p-value=0.39). These observations indicate uncorrelated coding mechanisms for SF and category in both single and population-level representations in the IT cortex.

Next, to investigate SF and category coding characteristics, we systematically removed individual neurons from the population and measured the resulting drop in LDA classifier accuracy as a metric for the neuron's impact, termed single neuron contribution (SNC). **Figure 5a** illustrates the SNC score for SF (two labels, LSF (R1 and R2) vs. HSF (R4 and R5)) and category (face vs. non-face) decoding within 70ms to 170ms after the stimulus onset. The SNC in SF is significantly higher than for category (average SNC for SF=0.51%±0.02 and category=0.1%±0.04, SF > category with p-value=1.6×1.6^{-13}). Therefore, SF representation relies more on individual neuron representations, suggesting a sparse mechanism of SF coding where single-level neuron information is less redundant. In contrast, single-level representations of category appear to be more redundant and robust against information loss or noise at the level of individual neurons. We utilized conditional mutual information (CMI) between pairs of neurons conditioned on the label, SF (LSF (R1 and R2) vs. HSF (R4 and R5)) or category, to assess the information redundancy across the neurons. CMI quantifies the shared information between the population of two neurons regarding SF or category coding. **Figure 5b** indicates a significantly lower CMI for SF (average CMI for SF=0.66±0.0009 and category=0.69±0.0007, SF<category with p-value0), indicating that neurons carry more independent SF-related information than category-related information.

To investigate each neuron's contribution to the decoding procedure (LDA decision), we computed the sparseness of the LDA weights corresponding to each neuron (see Materials and methods). For SF, we trained the LDA on R1, R2, R4, and R5 with two labels (one for R1 and R2 and the alternative for R4 and R5). A second LDA was trained to discriminate between faces and non-faces. Subsequently, we calculated the sparseness of the weights associated with each neuron in SF and category decoding. **Figure 5c** illustrates the time course of the weight sparseness for SF and category. The category reflects a bimodal curve with the first peak at 110ms and the second at 210ms after stimulus onset. The second peak is significantly larger than the first one (category first peak, 0.016±0.007, second peak, 0.051±0.013, and p-value<0.001). In SF decoding, neurons' weights exhibit a trimodal curve with peaks at 100ms, 215ms, and 320ms after the stimulus onset. The first peak is significantly higher than the other two (SF first peak, 0.038±0.005, second peak, 0.018±0.003, third peak, 0.028±0.003, first peak > second peak with p-value<0.001, and first peak > third peak with p-value=0.014). Comparing SF and category, during the early phase of the response (70ms to 170ms), SF sparseness is higher, while in 170ms to 270ms, the sparseness value of the category is higher (p-value < 0.001 for both time intervals). This suggests that, initially, most neurons contribute to category representation, but later, the majority of neurons are involved in SF coding. These findings support distinct mechanisms governing SF and category coding in the IT cortex.

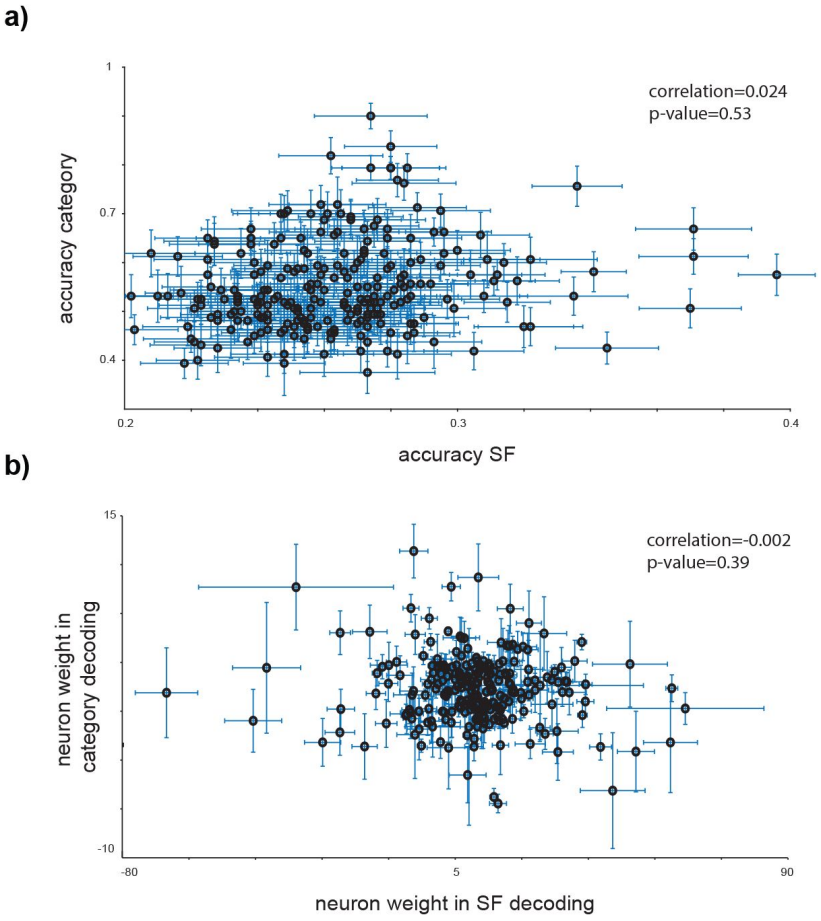

Figure 4.

Uncorrelated mechanisms for SF and category coding.

a *uncorrelated SF and category coding in the single level*. The scatter plot indicates the category-SF accuracies and does not reveal a significant correlation between SF and category coding capabilities within the IT cortex at the single-neuron level. The error bars show the STD for SF and category decoding accuracies. **b** *uncorrelated neuron contribution in SF and category coding in population*. The LDA weight of each neuron is considered as the neuron contribution in the population coding of SF or category (see Materials and methods). The scatter plot of the neuron weights in SF shows a near-zero correlation with the neuron weights in category coding.

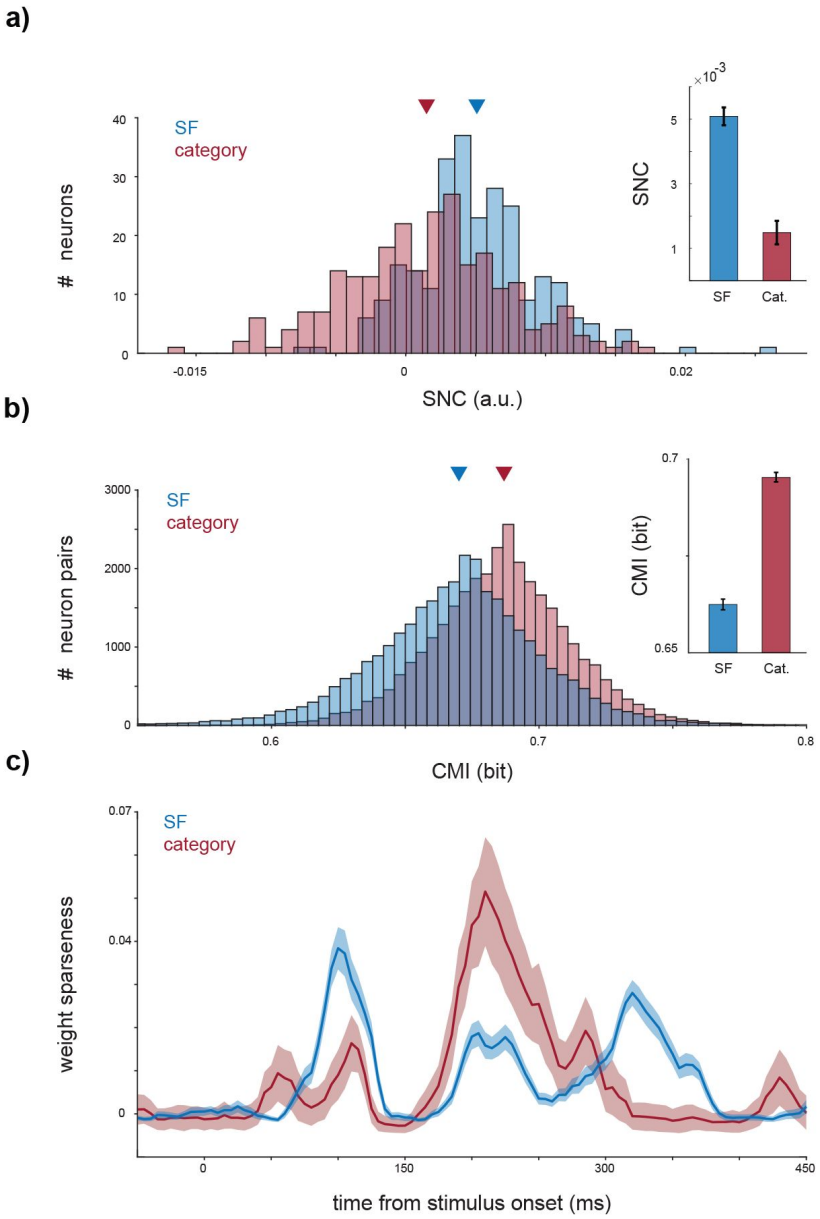

Figure 5.

Sparse SF coding compared to category coding.

a,**b** *Sparse mechanism for SF coding*. **a** The contribution of each neuron in SF and category (face vs. non-face) decoding is evaluated by removing it from the feature set fed to the LDA within the time window of 70ms to 170ms after stimulus onset. The histogram of the SNC value (see Materials and methods) is presented, indicating the amount of accuracy loss when a neuron is removed. The bar plot displays the average SNC values for SF and category, with error bars representing the SEM. The SNC value for SF is significantly higher than for the category. **b** Furthermore, the CMI of each neuron pair, conditioned to the label (category or SF), is illustrated. CMI reflects the information redundancy between neuron pairs during SF or category decoding. A lower CMI value for SF indicates that individual neurons carry more independent SF-related information compared to category information. **c** *Sparse neuron contribution in SF coding at the early phase of the response*. To investigate the contribution of the neurons in population decoding, the sparseness of the LDA weights assigned to each neuron is calculated. Higher sparseness indicates a greater contribution of a smaller group of neurons to the decoding process. The time course of weight sparseness is depicted for SF and category (face vs. non-face) decoding, with shadows representing the STD. During the early phase of the response, the sparseness of SF-related weights is higher than that of the category, while this relationship is reversed during the late phase of the response.

SF representation in the artificial neural networks

We conducted a thorough analysis to compare our findings with CNNs. To assess the SF coding capabilities of CNNs, we utilized popular architectures, including ResNet18, ResNet34, VGG11, VGG16, InceptionV3, EffcientNetb0, CORNet-S, CORTNet-RT, and CORNet-z, with both pre-trained on ImageNet and randomly initialized weights (see Materials and methods). Employing feature maps from the four last layers of each CNN, we trained an LDA model to classify the SF content of input images. The results indicated that CNNs exhibit SF coding capabilities with much higher accuracies than the IT cortex. **Figure 6a** shows the SF decoding accuracy of the CNNs on our dataset (SF decoding accuracy with random (R) and pre-trained (P) weights, ResNet18: P=0.96±0.01 / R=0.94±0.01, ResNet34 P=0.95±0.01 / R=0.86±0.01, VGG11: P=0.94±0.01 / R=0.93±0.01, VGG16: P=0.92±0.02 / R=0.90±0.02, InceptionV3: P=0.89±0.01 / R=0.67±0.03, EffcientNetb0: P=0.94±0.01 / R=0.30±0.01, CORNet-S: P=0.77±0.02 / R=0.36±0.02, CORTNet-RT: P=0.31±0.02 / R=0.33±0.02, and CORNet-z: P=0.94±0.01 / R=0.97±0.01). Except for CORNet-z, object recognition training increases the network's capacity for SF coding, with an improvement as significant as 64% in EffcientNetb0. Furthermore, except for the CORNet family, LSF content exhibits higher recall values than HSF content, as observed in the IT cortex (p-value with random (R) and pre-trained (P) weights, ResNet18: P=0.39 / R=0.06, ResNet34 P=0.01 / R=0.01, VGG11: P=0.13 / R=0.07, VGG16: P=0.03 / R=0.05, InceptionV3: P=<0.001 / R=0.05, EffcientNetb0: P=0.07 / R=0.01). The recall values of CORNet-Z and ResNet18 are illustrated in **Figure 6b**. However, while the CNNs exhibited some similarities in SF representation with the IT cortex, they did not replicate the SF-based profiles that predict neuron category selectivity. As depicted in **Figure 6c**, although neurons formed similar profiles, these profiles were not associated with the category decoding performances of the neurons sharing the same profile.

Discussion

Utilizing neural responses from the IT cortex of passive-viewing monkeys, we conducted a study on SF representation within this pure visual high-level area. Numerous psychophysical studies have underscored the significant impact of SF on object recognition, highlighting the importance of its representation. To the best of our knowledge, this study presents the first attempt to systematically examine the SF representation in a high-level area, i.e., the IT cortex, using extracellular recording. Understanding SF representation is crucial, as it can elucidate the object recognition procedure in the IT cortex.

Our findings demonstrate explicit SF coding at both the single-neuron and population levels, with LSF being decoded faster and more accurately than HSF. During the early phase of the response, we observe a preference for LSF, which shifts toward a preference for HSF during the late phase. Next, we made profiles based on SF-only (phase-scrambled stimuli) responses for each neuron to predict its category selectivity. Our results show a direct relationship between the population's category coding capability and the SF coding capability of individual neurons. While we observed a relation between SF and category coding, we have found uncorrelated representations. Unlike category coding, SF relies more on sparse, individual neuron representations. Finally, when comparing the responses of IT with those of CNNs, it is evident that while SF coding exists in CNNs, the SF profile observed in the IT cortex is notably absent. Our results are based on grouping the neurons of the two monkeys; however, the results remain consistent when looking at the data from individual monkeys as illustrated in Appendix 2.

The influence of SF on object recognition has been extensively investigated through psychophysical studies (Joubert et al., 2007; Schyns and Oliva, 1994; Craddock et al., 2013; Caplette et al., 2014; Cheung and Bar, 2014; Ashtiani et al., 2017). One frequently explored theory is the coarse-to-fine nature of SF processing in object recognition (Schyns and Oliva, 1994;

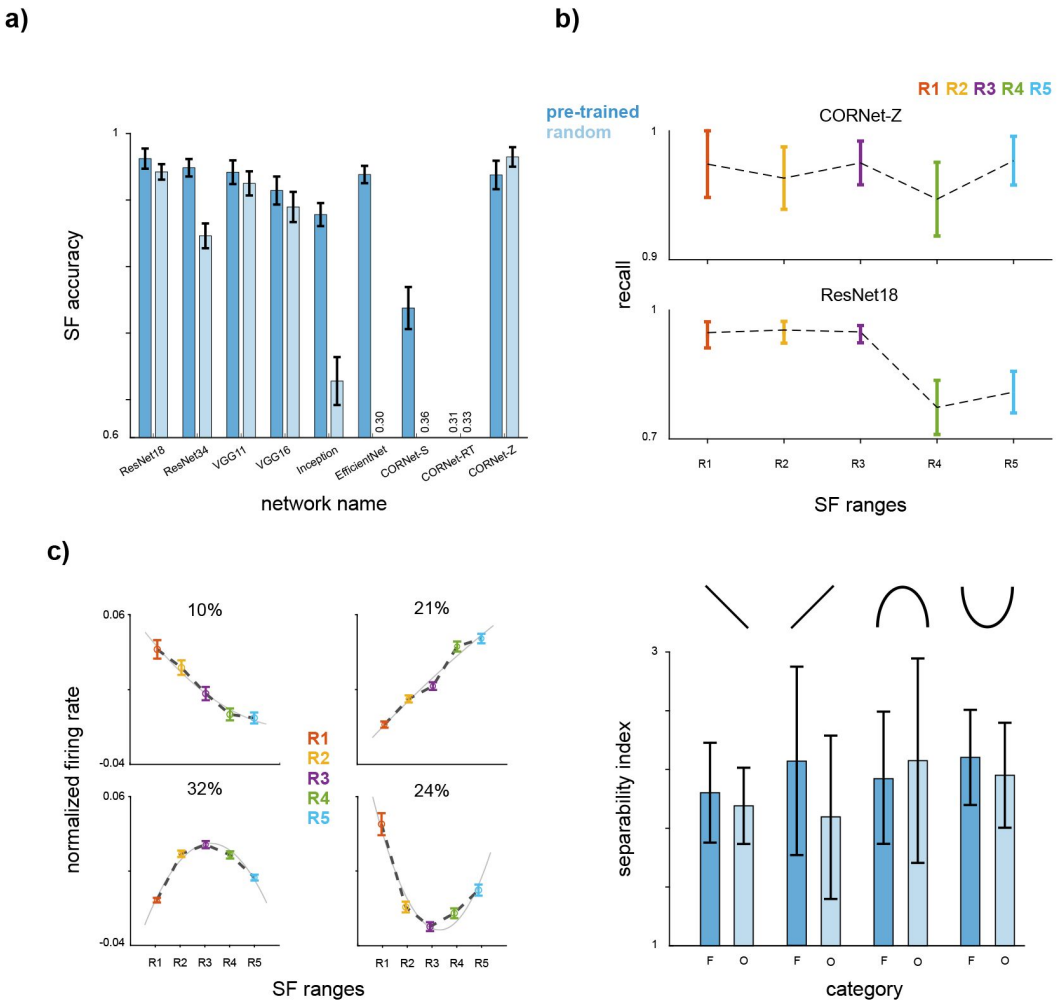

Figure 6.

SF representation in CNNs.

a *SF coding capabilities*. We assessed the SF coding capabilities of popular CNN architectures (ResNet18, ResNet34, VGG11, VGG16, InceptionV3, EffcientNetb0, CORNet-S, CORTNet-RT, and CORNet-z) using both randomly initialized (R) and pre-trained (P) weights on ImageNet. An LDA model was trained using feature maps from the four last layers of each CNN to classify the SF content of input images. The SF decoding accuracy for each CNN on our dataset is presented with error bars indicating the STD. **b** *LSF-preferred recall performance*. The recall performance of two sample networks (CORNET-z and ResNet18) is presented. STD values are illustrated with error bars. The recall values for LSF content were higher than HSF content in most CNNs, resembling the trends observed in the IT cortex. **c** The profiles (left) and face/non-face SI value (right) of a sample network (ResNet18). Profiles are calculated similarly to the IT cortex. CNNs did not replicate the SF-based profiles observed in the IT cortex.

Rotshtein et al., 2010; Gao, 2011; Yardley et al., 2012; Kauffmann et al., 2015; Rokszin, 2016). This aligns with our observation that the onset of LSF is significantly lower than HSF. Different SF bands carry distinct information, progressively conveying coarse-to-fine shape details as we transition from LSF to HSF. Psychophysical studies have indicated the utilization of various SF bands for distinct categorization tasks (Rotshtein et al., 2010). Considering the face as a behaviorally demanded object, psychophysical studies have observed the influence of various SF bands on face recognition. These studies consistently show that enhanced face recognition performance is achieved in the middle and higher SF bands compared to LSF (Costen et al., 1996; Hayes et al., 1986; Fiorentini et al., 1983; Cheung et al., 2008; Awasthi, 2012; Jeantet, 2019). These observations resonate with the identified SF profiles in our study. Neurons that exhibit heightened responses as SF shifts towards HSF demonstrate superior coding of faces compared to other neuronal groups.

Unlike psychophysical studies, imaging studies in this area have been relatively limited. Gaska et al. (1988) observed low-pass tuning curves in the V3A area, and Chen et al. (2018) reported an average low-pass tuning curve in the superior colliculus (SC). Purushothaman et al. (2014) identified two distinct types of neurons in V1 based on their response to SF. The majority of neurons in the first group exhibited a monotonically shifting preference toward HSF over time. In contrast, the second group showed an initial increase in preferred SF followed by a decrease. Our findings align with these observations, showing a rise in preferred SF starting at 170ms after stimulus on-set, followed by a decline at 220ms after stimulus onset. Additionally, Zhang et al. (2023) found that LSF is the preferred band for over 40% of V4 neurons. This finding is also consistent with our observations, where approximately 40% of neurons consistently exhibited the highest firing rates in response to LSF throughout all response phases. Collectively, these results suggest that the average LSF preferred tuning curve observed in the IT cortex could be a characteristic inherited from the lower areas in the visual hierarchy. Moreover, examining the course-to-fine theory of SF processing, Chen et al. (2018) and Purushothaman et al. (2014) observed a faster response to LSF compared to HSF in SC and V1, which resonates with our course-to-fine observation in SF decoding. When analyzing the relationship between the SF content of complex stimuli and IT responses, Bermudez et al. (2009) observed a correlation between neural responses in the IT cortex and the SF content of the stimuli. This finding is in line with our observations, as decoding results directly from the distinct patterns exhibited by various SF bands in neural responses.

To rule out the degraded contrast sensitivity of the visual system to medium and high SF information because of the brief exposure time, we repeated the analysis with 200ms exposure time as illustrated in **Appendix 1 - Figure 4** which indicates the same LSF-preferred results. Furthermore, according to **Figure 2**, the average firing rate of IT neurons for HSF could be higher than LSF in the late response phase. It indicates that the amount of HSF input received by the IT neurons in the later phase is as much as LSF, however, its impact on the IT response is observable in the later phase of the response. Thus, the LSF preference is because of the temporal advantage of the LSF processing rather than contrast sensitivity. Next, according to **Figure 3(a)**, 6% of the neurons are HSF-preferred and their firing rate in HSF is comparable to the LSF firing rate in the LSF-preferred group. This analysis is carried out in the early phase of the response (70-170ms). While most of the neurons prefer LSF, this observation shows that there is an HSF input that excites a small group of neurons. Additionally, the highest SI belongs to the HSF-preferred profile in the early phase of the response which supports the impact of the HSF part of the input. Similar LSF-preferred responses are also reported by Chen et al. (2018) (50ms for SC) and Zhang et al. (2023) (3.5 - 4 secs for V2 and V4). Therefore, our results show that the LSF-preferred nature of the IT responses in terms of firing rate and recall, is not due to the weakness or lack of input source (or information) for HSF but rather to the processing nature of the SF in the IT cortex.

Hong et al. (2016) suggested that the neural mechanisms responsible for developing tolerance to identity-preserving transform also contribute to explicitly representing these category-orthogonal transforms, such as rotation. Extending this perspective to SF, our results similarly suggest an explicit representation of SF within the IT population. However, unlike transforms such as rotation, the neural mechanisms in IT leverage various SF bands for various categorization tasks. Furthermore, our analysis introduced a novel SF-only profile for the first time predicting category selectivity.

These findings prompt the question of why the IT cortex explicitly represents and codes the SF content of the input stimuli. In our perspective, the explicit representation and coding of SF contents in the IT cortex facilitates object recognition. The population of the neurons in the IT cortex becomes selective for complex object features, combining SFs to transform simple visual features into more complex object representations. However, the specific mechanism underlying this combination is yet to be known. The diverse SF contents present in each image carry valuable information that may contribute to generating expectations in predictive coding during the early phase, thereby facilitating information processing in subsequent phases. This top-down mechanism is suggested by the works of Bar (2003) and Fenske et al. (2006).

Moreover, each object has a unique "characteristic SF signature," representing its specific arrangement of SFs. "Characteristic SF signatures" refer to the unique patterns or profiles of SFs associated with different objects or categories of objects. When we look at visual stimuli, such as objects or scenes, they contain specific arrangements of different SFs. Imagine a scenario where we have two objects, such as a cat and a car. These objects will have different textures and shapes, which correspond to different distributions of SFs. The cat, for instance, might have a higher concentration of mid-range SFs related to its fur texture, while the car might have more pronounced LSFs that represent its overall shape and structure. The IT cortex encodes these signatures, facilitating robust discrimination and recognition of objects based on their distinctive SF patterns.

The concept of "characteristic SF signatures" is also related to the "SF tuning" observed in our results. Neurons in the visual cortex, including the IT cortex, have specific tuning preferences for different SFs. Some neurons are more sensitive to HSF, while others respond better to LSF. This distribution of sensitivity allows the visual system to analyze and interpret different information related to different SF components of visual stimuli concurrently. Moreover, the IT cortex's coding of SF can contribute to object invariance and generalization. By representing objects in terms of their SF content, the IT cortex becomes less sensitive to variations in size, position, or orientation, ensuring consistent recognition across different conditions. SF information also aids the IT cortex in categorizing objects into meaningful groups at various levels of abstraction. Neurons can selectively respond to shared SF characteristics among different object categories (assuming that objects in the same category share a level of SF characteristics), facilitating decision-making about visual stimuli. Overall, we posit that SF's explicit representation and coding in the IT cortex enhance its proficiency in object recognition. By capturing essential details and characteristics of objects, the IT cortex creates a rich representation of the visual world, enabling us to perceive, recognize, and interact with objects in our environment.

Finally, we compared SF's representation within the IT cortex and the current state of the art networks in deep neural networks. CNNs stand as one of the most promising models for comprehending visual processing within the primate ventral visual processing stream (Kubilius et al., 2018, 2019). Examining the higher layers of CNN models (most similar to IT), we found that randomly initialized and pre-trained CNNs can code for SF. This is consistent with our previous work on the CIFAR dataset (Toosi et al., 2022). Nevertheless, they do not exhibit the SF profile we observed in the IT cortex. This emphasizes the uniqueness of SF coding in the IT cortex and suggests that artificial neural networks might not fully capture the complete complexity of biological visual processing mechanisms, even when they encompass certain aspects of SF

representation. Our results intimate that the IT cortex uses a different mechanism for SF coding compared to contemporary deep neural networks, highlighting the potential for innovating new approaches to consider the role of SF in the ventral stream models.

Our results are not affected by several potential confounding factors. First, each stimulus in the set also has a corresponding phase-scrambled variant. These phase-scrambled stimuli maintain the same SF characteristics as their respective face or non-face counterparts but lack shape information. This approach allows us to investigate SF representation in the IT cortex without the confounding influence of shape information. Second, our results, obtained through a passive viewing task, remain unaffected by attention mechanisms. Third, All stimuli (intact, SF filtered, and phase scrambled) are corrected for illumination and contrast to remove the attribution of the category-orthogonal basic characteristics of stimuli into the results (see Materials and methods). Fourth, while our dataset does not exhibit a balance in samples per category, it is imperative to acknowledge that this imbalance does not exert an impact on our observed outcomes. We have equalized the number of samples per category when training our classification models by random sampling from the stimulus set (see Materials and methods). One limitation of our study is the relatively low number of objects in the stimulus set. However, the decoding performance of category classification (face vs. non-face) in intact stimuli is 94.2%. The recall value for objects vs. scrambled is 90.45%, and for faces vs. scrambled is 92.45 (p-value=0.44), which indicates the high level of generalizability and validity characterizing our results. Finally, since our experiment maintains a fixed SF content in terms of both cycles per degree and cycles per image, further experiments are needed to discern whether our observations reflect sensitivity to cycles per degree or cycles per image.

In summary, we studied the SF representation within the IT cortex. Our findings reveal the existence of a sparse mechanism responsible for encoding SF in the IT cortex. Moreover, we studied the relationship between SF representation and object recognition by identifying an SF profile that predicts object recognition performance. These findings establish neural correlates of the psychophysical studies on the role of SF in object recognition and shed light on how IT represents and utilizes SF for the purpose of object recognition.

Materials and methods

Animals and recording

The activity of neurons in the IT cortex of two male macaque monkeys weighing 10 and 11 kg, respectively, was analyzed following the National Institutes of Health Guide for the Care and Use of Laboratory Animals and the Society for Neuroscience Guidelines and Policies. The experimental procedures were approved by the Institute of Fundamental Science committee. Before implanting a recording chamber in a subsequent surgery, magnetic resonance imaging and Computed Tomography (CT) scans were performed to locate the prelunate gyrus and arcuate sulcus. The surgical procedures were carried out under sterile conditions and Isoflurane anaesthesia. Each monkey was fitted with a custom-made stainless-steel chamber, secured to the skull using titanium screws and dental acrylics. A craniotomy was performed within the 30x70mm chamber for both monkeys, with dimensions ranging from 5 mm to 30 mm A/P and 0 mm to 23 mm M/L.

During the experiment, the monkeys were seated in custom-made primate chairs, and their heads were restrained while a tube delivered juice rewards to their mouths. The system was mounted in front of the monkey, and eye movements were captured at 2KHz using the EyeLink PM-910 Illuminator Module and EyeLink 1000 Plus Camera (SR Research Ltd, Ottawa, CA). Stimulus presentation and juice delivery were controlled using custom software written in MATLAB with the MonkeyLogic toolbox. Visual stimuli were presented on a 24-inch LED-lit monitor

(AsusVG248QE, 1920 × 1080, 144 Hz) positioned 65.5 cm away from the monkeys' eyes. The actual time the stimulus appeared on the monitor was recorded using a photodiode (OSRAM Opto Semiconductors, Sunnyvale, CA).

One electrode was affxed to a recording chamber and positioned within the craniotomy area using the Narishige two-axis platform, allowing for continuous electrode positioning adjustment. To make contact with or slightly penetrate the dura, a 28-gauge guide tube was inserted using a manual oil hydraulic micromanipulator from Narishige, Tokyo, Japan. For recording neural activity extracellularly in both monkeys, varnish-coated tungsten microelectrodes (FHC, Bowdoinham, ME) with a shank diameter of 200–250 μm and impedance of 0.2–1 Mw (measured at 1kHz) were inserted into the brain. A pre-amplifier and amplifier (Resana, Tehran, Iran) were employed for single-electrode recordings, with filtering set between 300 Hz and 5 KHz for spikes and 0.1 Hz and 9 KHz for local field potentials. Spike waveforms and continuous data were digitized and stored at a sampling rate of 40 kHz for offline spike sorting and subsequent data analysis. Area IT was identified based on its stereotaxic location, position relative to nearby sulci, patterns of gray and white matter, and response properties of encountered units.

Stimulus and task paradigm

The experimental task comprised two distinct phases

selectivity and main phases, each involving different stimuli. During the selectivity phase, the objective was to identify a responsive neuron for recording purposes. If an appropriate neuron was detected, the main phase was initiated. However, if a responsive neuron was not observed, the recording location was adjusted, and the selectivity phase was repeated. First, we will outline the procedure for stimulus construction, followed by an explanation of the task paradigm.

The stimulus set

The size of each image was 500 × 500 pixels. Images were displayed on a 120 Hz monitor with a resolution of 1920 × 1080 pixels. The monitor's response time (changing the color of pixels in grey space) was one millisecond. The monkey's eyes were located at a distance of 65cm from the monitor. Each stimulus occupied a space of 5 × 5 degrees. All images were displayed in the center of the monitor. During the selectivity phase, a total number of 155 images were used as stimuli. Regarding SF, the stimuli were divided into unfiltered and filtered categories. Unfiltered images included 74 separate grayscale images in the categories of animal face, animal body, human face, human body, man-made and natural. To create the stimulus, these images were placed on a grey background with a value of 0.5. The filtered images included 27 images in the same categories as the previous images, which were filtered in two frequency ranges (along with the intact form): low (1 to 10 cycles per image) and high (18 to 75 cycles per image), totaling 81 images. In the main phase of the test, nine images, including three non-face images and six face images, were considered. These images were displayed in **Figure 1c**. For the main phase, the images were filtered in five frequency ranges. These intervals were 1 to 5, 5 to 10, 10 to 18, 18 to 45, and 45 to 75 cycles per image. For each image in each frequency range, a scrambled version had been obtained by scrambling the image phase in the Fourier transforms domain. Therefore, each image in the main phase contained one unfiltered version (intact), five filtered versions (R1 to R5), and six scrambled versions (i.e., 12 versions in total).

SF filtering

Butterworth filters were used to filter the images in this study. A low-pass Butterworth filter is defined as follows.

$$B_{lp}(r, f_c) = \frac{1}{1 + (r/f_c)^{2n}} \quad (1)$$

where B_{lp} is the absolute value of the filter, r is the distance of the pixel from the center of the image, f_c is the filter's cutoff frequency in terms of cycles per image, and n is the order of the filter. Similarly, the high-pass filter is defined as follows.

$$B_{hp}(r, f_c) = \frac{1}{1 + (f_c/r)^{2n}} \quad (2)$$

To create a band-pass filter with a pass frequency of f_1 and a cutoff frequency of f_2, a multiplication of a high-pass and a low-pass filter was performed ($B_{bp}(r, f_1, f_2) = B_{lp}(r; f_1) \times B_{hp}(r; f_2)$). To apply the filter, the image underwent a two-dimensional Fourier transform, followed by multiplication with the appropriate filter. Subsequently, the inverse Fourier transform was employed to obtain the filtered image. Afterward, a linear transformation was applied to adjust the brightness and contrast of the images. Brightness was determined by the average pixel value of the image, while contrast was represented by its standard deviation (STD). To achieve specific brightness (L) and contrast (C) levels, the following equation was employed to correct the images.

$$I_{norm} = C \times \left(\frac{I - \mu}{\sigma} \right) + L \quad (3)$$

where $<Y$ and μ are the STD and mean of the image. In this research, specific values for L and C were chosen as 0.5 (corresponding to 128 on a scale of 255) and 0.0314 (equivalent to 8 on a scale of 255), respectively. Analysis of Variance (ANOVA) indicated no significant difference in brightness and contrast among various groups, with p-values of 0.62 for brightness and 0.25 for contrast. Finally, we equalized the stimulus power in all SF bands (intact, R-R5). The SF power among all conditions (all SF bands, face vs. non-face and unscrambled vs. scrambled) does not vary significantly (ANOVA, p-value>0.1). SF power is calculated as the sum of the square value of the image coeffcients in the Fourier domain. To create scrambled images, the original image underwent Fourier transformation, after which its phase was scrambled. Subsequently, the inverse Fourier transform was applied. Since the resulting signal may not be real, its real part was extracted. The resulting image then underwent processing through the specified filters in the primary phase.

Task paradigm

The task was divided into two distinct phases: the selectivity phase and the main phase. Each phase comprised multiple blocks, each containing two components: the presentation of a fixation point and a stimulus. The monkey was required to maintain fixation within a window of ±1.5 degrees around the center of the monitor throughout the entire task. During the selectivity phase, there were five blocks, and stimuli were presented randomly within each block. The duration of stimulus presentation was 50ms, while the fixation point was presented for 500ms. The selectivity phase consisted of a total of 775 trials. A neuron was considered responsive if it exhibited a significant increase in response during the time window of 70ms to 170ms after stimulus onset, compared to a baseline window of -50ms to 50ms. This significance was determined using the Wilcoxon signed-rank test with a significance level of 0.05. Once a neuron was identified as responsive, the main phase began. In the main phase, there were 15 blocks. The main phase involved a combination of the six most responsive stimuli, selected from the selectivity phase, along with nine fixed stimuli. There was, on average, 7.54 face stimulus in each session. In each block, all stimuli were presented once in random order. The stimulus duration in the main phase was 33ms, and the fixation point was presented for 465ms. For the purpose of analysis, our focus was primarily on the main phase of the task.

Neural representation

All analyses were conducted using custom code developed in Matlab (MathWorks). In total, 266 neurons (157 M1 and 109 M2) were considered for the analysis. The recorded locations along with their SF and category selectivity is illustrated in Appendix 1 - **Figure 5**. Neurons were sorted using the ROSS toolbox (Toosi et al., 2021). Each stimulus in each time step was represented by a vector of N elements where the i'th element was the average response of the i'th neuron for that stimulus in a time window of 50ms around the given time step. We used both single-level and population-level analysis. Numerous studies had examined the benefits of population representation (Averbeck et al., 2006; Adibi et al., 2014; Abbott and Dayan, 1999; Dehaqani et al., 2018). These studies have demonstrated that enhancing signal correlation within the neural data population leads to improved decoding performance for object discrimination. To maintain consistency across trials, responses were normalized using the z-score procedure. All time courses were based on a 50ms sliding window with a 5ms time step. We utilized a time window from 70 ms to 170 ms after stimulus onset for our analysis (except for temporal analysis). This time window was selected because the average firing rate across neurons was significantly higher than the baseline window of -50 ms to 50 ms (Wilcoxon signed-rank test, p-value < 0.05).

Statistical analysis

All statistical analyses were conducted as outlined in this section unless otherwise specified. In the single-level analysis, where each run involves a single neuron, pair comparisons were performed using the Wilcoxon signed-rank test, and unpaired comparisons utilized the Wilcoxon rank-sum test, both at a significance level of 0.05. The results and their standard error of the mean (SEM) were reported. For population analysis, we used an empirical method, and the results were reported with their STD. To compare two paired sets of X and Y (Y could represent the chance level), we calculated the statistic r as the number of pairs where $x - y < 0$. The p-value was computed as r divided by the total number of runs, r/M, where M is the total number of runs. When $r = 0$, we used the notation of p-value<1/M.

Classification

All classifications were carried out employing the LDA method, both in population and single level. As described before, each stimulus in each block was shown by an N-element vector to be fed to the classifier. For face (non-face) vs. scrambled classification, only the face (non-face) and scrambled intact stimuli were used. For face vs. non-face (category) classification, only unscrambled intact stimuli were utilized. Finally, only the scrambled stimuli were fed to the classifier for the SF classification, and the labels were SF bands (R1, R2, ..., R5, multi-label classifier). In population-level analysis, averages and standard deviations were computed using a leave-p-out method, where 30% of the samples were kept as test samples in each run. All analyses were based on 1000 leave-p-out runs. To determine the onset time, one STD was added to the average accuracy value in the interval of 50ms before to 50ms after stimulus onset. Then, the onset time was identified as the point where the accuracy was significantly greater than this value for five consecutive time windows.

Preferred SF

Preferred SF for a given neuron was calculated as follows,

$$PSF = \sum_i (f_{Ri} \times c_{Ri}) / \sum_i f_{Ri} \quad (4)$$

where $P\,SF$ is the preferred SF, f_{Ri} is the average firing rate of the neuron for Ri, and c_{Ri} is −2 for R1, −1 for R2, ..., 2 for R5. When $P\,SF > 0$, the neuron exhibits higher firing rates for higher SF ranges on average and vice versa. To identify the number of neurons responding to a specific SF

range higher than others, we performed an ANOVA analysis with a significance level of 0.05. Then, we picked the SF range with the highest firing rate for that neuron.

SF profile

To form the SF profiles, a quadratic curve was fitted to the neuron response from R1 to R5, using exclusively scrambled stimuli. Each trial was treated as an individual sample. Neurons were categorized into three groups based on the extremum point of the fitted curve: i) extremum is lower than R2, ii) between R2 and R4, and iii) greater than R4. Within the first group, if the neuron's response in R1 and R2 significantly exceeded (or fell below) R4 and R5, the SF profile was classified as LSF preferred (or HSF preferred). The same procedure went for the third group. Considering the second group, if the neuron response in R2 was significantly (Wilcoxon signed-rank) higher (or lower) than the response of R1 and R5, the neuron profile identified as U (or IU). Neurons not meeting any of these criteria were grouped under the flat category.

To establish sub-populations of SF/category-sorted neurons, we initially sorted the neurons according to their accuracy to decode the SF/category. Subsequently, a sliding window of size 20 was employed to select adjacent neurons in the SF or category-sorted list. Consequently, the first sub-population comprised the initial 20 neurons exhibiting the lowest individual accuracy in decoding the SF/category. In comparison, the last sub-population encompassed the top 20 neurons with the highest accuracy in decoding SF/category.

Separability Index

The discrimination of two or more categories, as represented by the responses of the IT population, can be characterized through the utilization of the scatter matrix of category members. The scatter matrix serves as an approximate measure of covariance within a high-dimensional space. The discernibility of these categories is influenced by two key components: the scatter within a category and the scatter between categories. SI is defined as the ratio of between-category scatter to within-category scatter. The computation of SI involves three sequential steps. Initially, the center of mass for each category, referred to as μ and the overall mean across all categories, termed the total mean, m, were calculated. Second, we calculated the between- and within-category scatters.

$$\begin{aligned} S_i &= \sum_{j,k \in C_i} (r_j - \mu_j)(r_k - \mu_k) \\ S_w &= \sum S_i \\ S_B &= \sum_{j,k \in C_i} n_i \times (\mu_i - m)(\mu_i - m) \end{aligned} \tag{5}$$

where S_i is the scatter matrix of the i'th category, r is the stimulus response, S_w is within-category scatter, S_B is the between-category scatter, and n_i is the number of samples in the i'th category.

Finally, SI was computed as

$$SI = \frac{\|S_B\|}{\|S_W\|} \tag{6}$$

where S indicates the norm of S. For additional information, please refer to the study conducted by Dehaqani et al. (2016).

SNC and CMI

To examine the influence of individual neurons on population-level decoding, we introduced the concept of the SNC. It measures the reduction in decoding performance when a single neuron is removed from the population. We systematically removed each neuron from the population one at a time and measured the corresponding drop in accuracy compared to the case where all neurons were present.

To quantify the CMI between pairs of neurons, we discretized their response patterns using ten levels of uniformly spaced bins. The CMI is calculated using the following formula.

$$CMI(n_i, n_j|c) = \sum_{n_i \in N_i, n_j \in N_j, c \in C} P(n_i, n_j, c) \times log_2 \frac{P(n_i, n_j|c)}{P(n_i|c) \times P(n_j|c)} \quad (7)$$

where n_i and n_j represent the discretized responses of the two neurons, and C represents the conditioned variable, which can be the category (face/non-face) or the SF range (LSF (R1 and R2) and HSF (R4 and R5)). We normalized the CMI by subtracting the CMI obtained from randomly shuffled responses and added the average CMI of SF and category. CMI calculation enables us to assess the degree of information shared or exchanged between pairs of neurons, conditioned on the category or SF while accounting for the underlying probability distributions.

Sparseness analysis

The sparseness analysis was conducted on the LDA weights, regarded as a measure of task relevance. To calculate the sparseness of the LDA weights, the neuron responses were first normalized using the z-score method. Then, the sparseness of the weights associated with the neurons in the LDA classifier was computed. The sparseness is computed using the following formula.

$$S = 1 - \frac{E(|w|)^2}{E(w^2)} \quad (8)$$

where w is the neuron weight in LDA, $E(w^2)$ represents the mean of the squared weights of the neurons. The maximum sparseness occurs when only one neuron is active, whereas the minimum sparseness occurs when all neurons are equally active.

Deep neural network analysis

To compare our findings with those derived from deep neural networks, we commenced by curating a diverse assortment of CNN architectures. This selection encompassed ResNet18, ResNet34, VGG11, VGG16, InceptionV3, EffcientNetb0, CORNet-S, CORTNet-RT, and CORNet-z, strategically chosen to offer a comprehensive overview of SF processing capabilities within deep learning models. Our experimentation spanned the utilization of both randomly initialized weights and pretrained weights sourced from the ImageNet dataset. This dual approach allowed us to assess the influence of prior knowledge embedded in pre-trained weights on SF decoding. In the process of extracting feature maps, we fed our stimulus set to the models, capturing the feature maps from the last four layers, excluding the classifier layer. Our results were primarily rooted in the final layer (preceding classification), yet they demonstrated consistency across all layers under examination. For classification and SF profiling, our methodology mirrored the procedures employed in our neural response analysis.

Appendix 1

Strength of SF selectivity

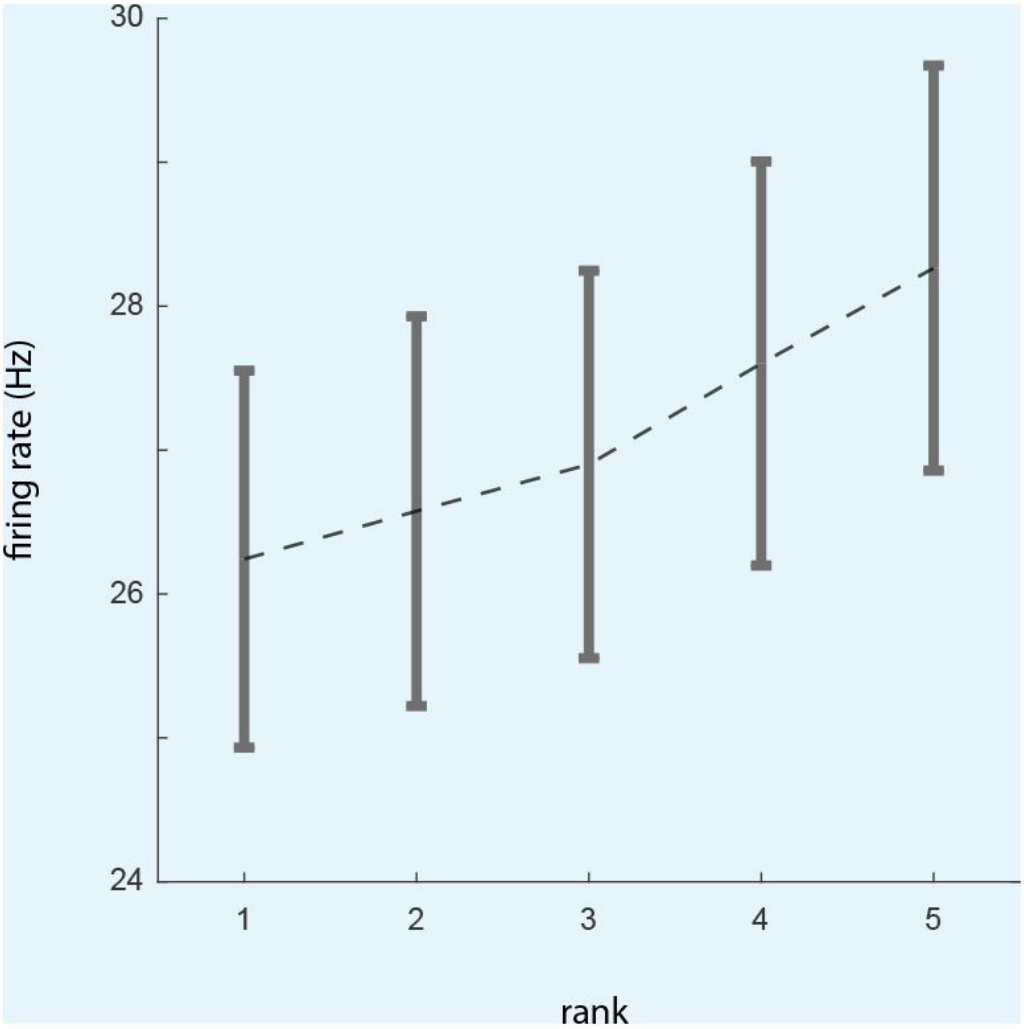

Appendix 1—figure 1.

Strength of SF selectivity

To asses the strength of SF selectivity in IT responses, we first ranked the SF content based on the firing rate in each neuron employing half of the trials. Then, the the other half is used to calculate the firing rate of each rank. Results show that the the firing rate of the rank 5 is significantly higher than rank 1 (p-value=4×10^{-4}).

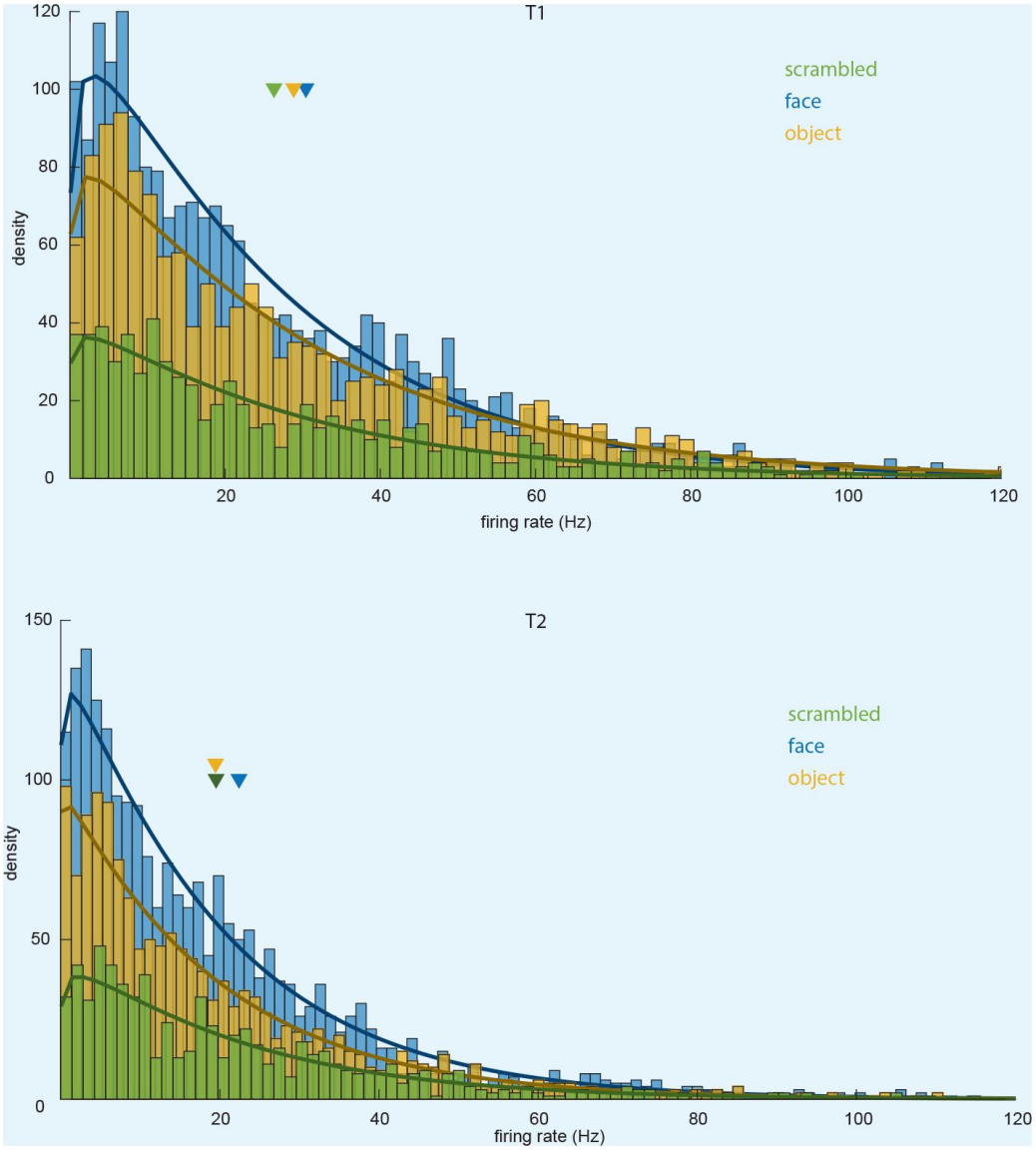

Appendix 1—figure 2.

SF response distribution

To check the SF response strength, the histogram of IT neuron responses to scrambled, face, and non-face stimuli is illustrated in this Figure. A Gamma distribution is also fitted to each histogram. To calculate the histogram, the neuron response to each unique stimulus is calculated for each neuron in spike/seconds (Hz). In the early phase, T1, the average firing rate to scrambled stimuli is 26.3 Hz which is significantly higher than the response in -50 to 50ms which is 23.4 Hz. In comparison, the mean response to intact face stimuli is 30.5 Hz, while non-face stimuli elicit an average response of 28.8 Hz. Moving to the late phase, T2, the responses to scrambled, face, and object stimuli are 19.5, 19.4, and 22.4 Hz, respectively.

Robustness of SF profiles

To investigate the robustness of the SF profiles, considering the trial-to-trial variability, we calculated the neuron's profile using half of the trials. Then, the neuron's response to R1, R2, …, R5 is calculated with the remaining trials. **Appendix 1 - Figure 3**, illustrates the average response of each profile for SF bands in each profile.

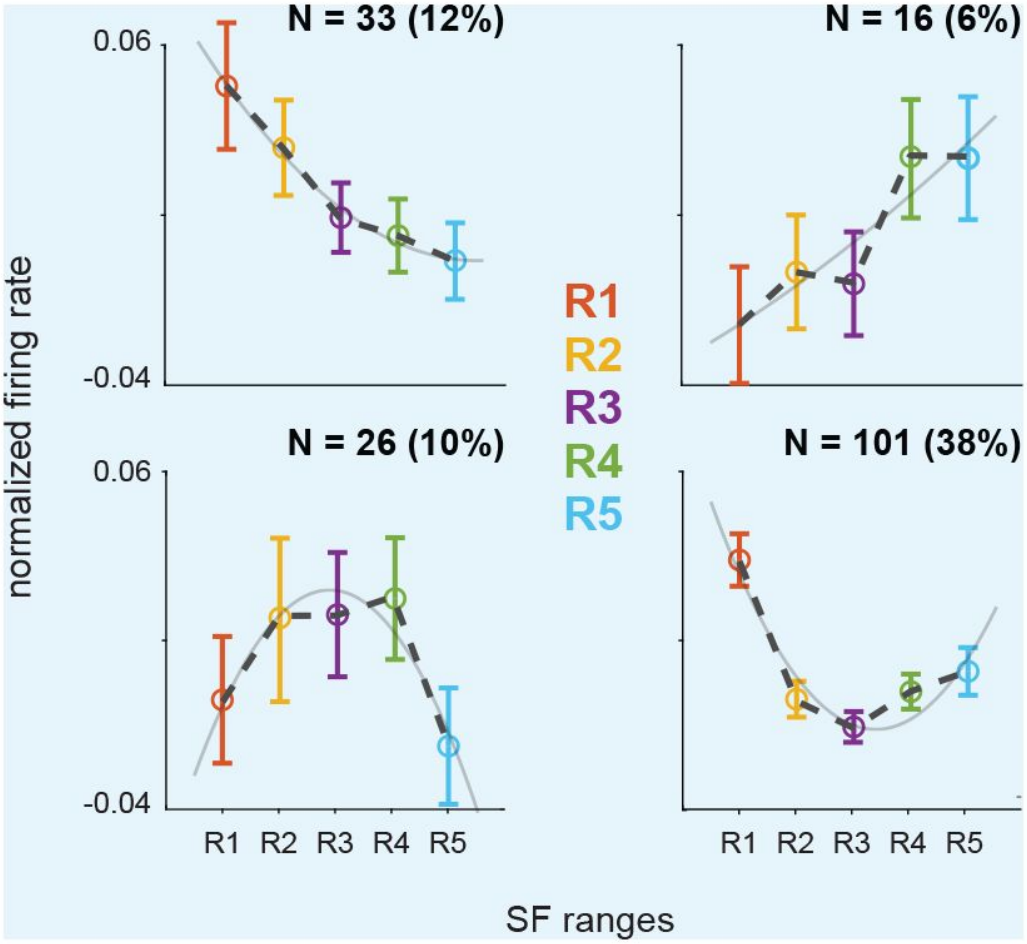

Appendix 1—figure 3.

SF profile robustness

Profiles are calculated using half of the trials. Then, the average of the neuron responses in each profile is calculated with the remaining half.

Extended stimulus duration supports LSF-preferred tuning

Our recorded data in the main phase contains the 200ms version of stimulus duration for all neurons. In this experiment, we investigate the impact of stimulus duration on LSF-preferred recall and course-to-fine nature of SF decoding. As illustrated in **Appendix 1 - Figure 4**, the LSF-preferred nature of SF decoding (recall R1=0.60±0.02, R2=0.44±0.03, R3=0.32 ±0.03, R4=0.35±0.03,

R5=0.36±0.02, and R1 > R5, p-value<0.001) and course-to-fine nature of SF processing (onset times in milliseconds after stimulus onset, R1=87.0±2.9, R2=86.0±4.0, R3=93.8±3.5, R4=96.1±3.9, R5=96.0±3.9, R1 < R5, p-value<0.001) is observed in extended stimulus duration. **a) b)**

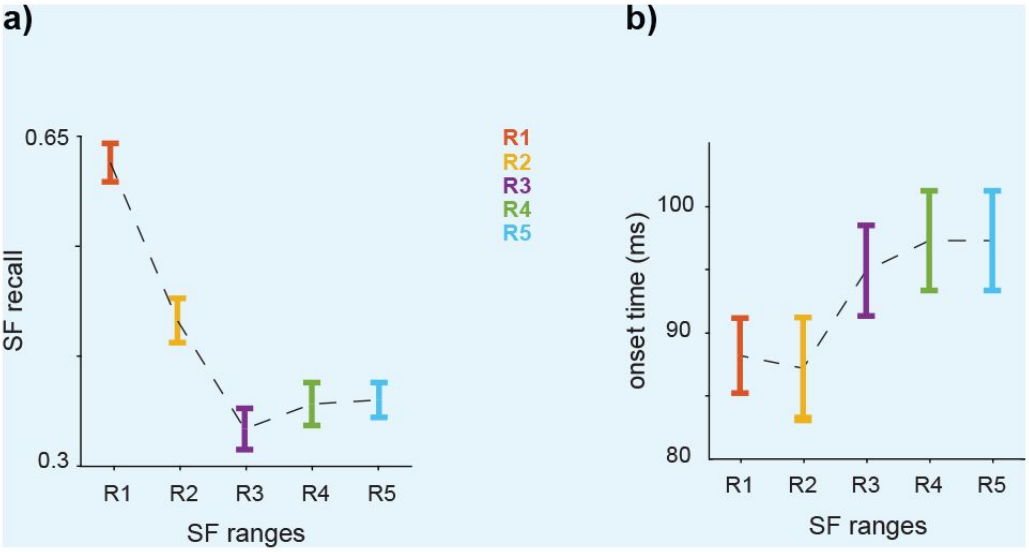

Appendix 1—figure 4.

LSF-preferred responses with extended stimulus duration

We conducted the experiments in **Appendix 1—Figure 1(e)** and **Appendix 1—Figure 2(a)** with 200ms of stimulus duration with the same method, in 70-170ms after stimulus onset. **a** The recall of each SF band in the population, as elicited by scrambled stimuli and determined through the LDA method, is presented. The error bars denote the STD. The findings support the LSF-preferred nature of SF decoding observed with 33ms of stimulus duration. **b** The onset time of recall for each spatial SF band in response to scrambled stimuli is depicted, with error bars representing the STD. The results imply an increasing onset time of decoding as SF values rise, as we observed in 33ms stimulus duration.

SF and Category selectivity based on the neuron's location

Appendix 1—figure 5.

The SF and category selectivity of the recorded locations

The accuracy of single neurons for SF prediction(**a**) and category prediction (**b**) is illustrated for each recorded location. x-axis and y-axis show anterior-posterior (A/P) or medial-lateral (M/L) hole location and the depth of the electrode in milliliters. A/P ranges from 5 mm (hole number 1) to 30 (hole number 18) mm and M/L ranges from 0 mm (hole number 1) to 23 mm (hole number 18).

Appendix 2

Main results for each monkey

In this section, we provide a summary of the main results for each monkey. **Appendix 1 - Figure 1** illustrates the key findings separately for M1 (157 neurons) and M2 (109 neurons). Regarding recall, both monkeys exhibit a decrease in recall values as the shift towards higher frequencies occurs (recall value for **M1:** R1=0.32±0.03, R2=0.30±0.02, R3=0.25±0.03, R4=0.24±0.03, and R5=0.24±0.03. **M2:** R1=0.60±0.03, R2=0.38±0.03, R3=0.29±0.03, R4= 0.35±0.03, and R5=0.35±0.03.). In both monkeys the recall value of R1 is significantly lower than R5 (for both M1 and M2, p-value < 0.001). In terms of onset, we observed a coarse-to-fine behavior in both monkeys (onset value in ms, **M1:** R1=84.7±5.5, R2=82.1±4.5, R3 =90.0±4.3, R4=86.8±7.0, R5=103.3±5.2. **M2:** R1=76.6±1.3, R2=76.0±1.2, R3=90.0±4.3, R4 =86.8±2.2, R5=89.0±1.9.). Next, we examined the SF-based profiles (**Figure 3**) in M1 and M2. As depicted in **Appendix 1 - Figure 1c**, both monkeys exhibit similar decoding capabilities in the SF-based profiles, consistent with what we observed in **Figure 3**. In both M1 and M2, face decoding significantly surpasses face/non-face decoding in all other profiles (**M1:** face SI: LP=0.23±0.05, HP=0.91±0.16, IU=0.06±0.03, U=0.14±0.02 / non-face, and HP > LP, U, IU with p-value < 0.001. Non-face SI:LP=0.13±0.07, HP=0.08±0.05, IU=0.16±0.09, U=0.19±0.10, and face SI in HP is greater than non-face SI in all profiles with p-value < 0.001. **M2:** face SI: LP=0.07±0.03, HP=0.38±0.18, IU=0.06±0.03, U=0.07±0.05 / non-face, and HP > LP, U, IU with p-value < 0.001. Non-face SI:LP=0.08±0.06, HP=0.03±0.03, IU=0.17±0.04, U=0.07±0.05, and face SI in HP is greater than non-face SI in all profiles with p-value < 0.001). Further-more, in both monkeys, the non-face decoding capability in IU is significantly higher than face decoding (p-value < 0.001).

Appendix 2—figure 1.

Main results for the two monkeys

The recall (**a**), onset of recall (**b**) and SI of each profile (**c**) is illustrated for M1 and M2, respectively. The results are consistent with our observations in *Results* section.

References

Abbott LF, Dayan P. (1999) **The effect of correlated variability on the accuracy of a population code** *Neural computation* **11**:91–101

Adibi M, McDonald JS, Clifford CW, Arabzadeh E. (2014) **Population decoding in rat barrel cortex: optimizing the linear readout of correlated population responses** *PLoS Computational Biology* **10**

Ashtiani MN, Kheradpisheh SR, Masquelier T, Ganjtabesh M. (2017) **Object categorization in finer levels relies more on higher spatial frequencies and takes longer** *Frontiers in psychology* **8**

Averbeck BB, Latham PE, Pouget A. (2006) **Neural correlations, population coding and computation** *Nature reviews neuroscience* **7**:358–366

Awasthi B. (2012) **Reach trajectories reveal delayed processing of low spatial frequency faces in developmental prosopagnosia** *Cognitive Neuroscience*

Bar M. (2003) **A cortical mechanism for triggering top-down facilitation in visual object recognition** *Journal of cognitive neuroscience* **15**:600–609

Bastin J, Vidal JR, Bouvier S, Perrone-Bertolotti M, Bénis D, Kahane P, David O, Lachaux JP, Epstein RA (2013) **Temporal 811 components in the parahippocampal place area revealed by human intracerebral recordings** *Journal of 812 Neuroscience* **33**:10123–10131

Bermudez MA, Vicente AF, Romero MC, Perez R, Gonzalez F. (2009) **Spatial frequency components influence cell activity in the inferotemporal cortex** *Visual neuroscience* **26**:421–428

Caplette L, West G, Gomot M, Gosselin F, Wicker B. (2014) **Affective and contextual values modulate spatial frequency use in object recognition** *Frontiers in psychology* **5**

Chaumon M, Kveraga K, Barrett LF, Bar M. (2014) **Visual predictions in the orbitofrontal cortex rely on associative content** *Cerebral cortex* **24**:2899–2907

Chen CY, Sonnenberg L, Weller S, Witschel T, Hafed ZM (2018) **Spatial frequency sensitivity in macaque midbrain** *Nature communications* **9**

Cheung OS, Bar M. (2014) **The resilience of object predictions: early recognition across viewpoints and exemplars** *Psychonomic bulletin & review* **21**:682–688

Cheung OS, Richler JJ, Palmeri TJ, Gauthier I. (2008) **Revisiting the role of spatial frequencies in the holistic processing of faces** *Journal of Experimental Psychology: Human Perception and Performance* **34**

Costen NP, Parker DM, Craw I. (1996) **Effects of high-pass and low-pass spatial filtering on face identification** *Perception & psychophysics* **58**:602–612

Craddock M, Martinovic J, Müller MM (2013) **Task and spatial frequency modulations of object processing: an EEG study** *PLoS One* **8**

Dehaqani MRA, Vahabie AH, Kiani R, Ahmadabadi MN, Araabi BN, Esteky H. (2016) **Temporal dynamics of visual category representation in the macaque inferior temporal cortex** *Journal of neurophysiology* **116**:587–831

Dehaqani MRA, Vahabie AH, Parsa M, Noudoost B, Soltani A. (2018) **Selective changes in noise correlations contribute 833 to an enhanced representation of saccadic targets in prefrontal neuronal ensembles** *Cerebral Cortex* **28**:3046–3063

Fenske MJ, Aminoff E, Gronau N, Bar M. (2006) **Top-down facilitation of visual object recognition: object-based and context-based contributions** *Progress in brain research* **155**:3–21

Fintzi AR, Mahon BZ (2014) **A bimodal tuning curve for spatial frequency across left and right human orbital frontal cortex during object recognition** *Cerebral Cortex* **24**:1311–1318

Fiorentini A, Maffei L, Sandini G. (1983) **The role of high spatial frequencies in face perception** *Perception* **12**:195–201

Gao Z. (2011) **Coarse-to-fine encoding of spatial frequency information into visual short-term memory for faces but impartial decay** *Journal of experimental psychology Human perception and performance*

Gaska JP, Jacobson LD, Pollen DA (1988) **Spatial and temporal frequency selectivity of neurons in visual cortical area V3A of the macaque monkey** *Vision research* **28**:1179–1191

Hayes T, Morrone MC, Burr DC (1986) **Recognition of positive and negative bandpass-filtered images** *Perception* **15**:595–602

Hong H, Yamins DL, Majaj NJ, DiCarlo JJ (2016) **Explicit information for category-orthogonal object properties increases along the ventral stream** *Nature neuroscience* **19**:613–622

Iidaka T, Yamashita K, Kashikura K, Yonekura Y. (2004) **Spatial frequency of visual image modulates neural responses 850 in the temporo-occipital lobe** *An investigation with event-related fMRI. Cognitive Brain Research* **18**:196–204

Jahfari S. (2013) **Spatial Frequency Information Modulates Response Inhibition and Decision-Making Processes** *PLoS ONE*

Jeantet C. (2019) **Time course of spatial frequency integration in face perception: An ERP study** *International journal of psychophysiology : offcial journal of the International Organization of Psychophysiology*

Joubert OR, Rousselet GA, Fize D, Fabre-Thorpe M. (2007) **Processing scene context: Fast categorization and object interference** *Vision research* **47**:3286–3297

Kauffmann L, Chauvin A, Guyader N, Peyrin C. (2015) **Rapid scene categorization: Role of spatial frequency order, accumulation mode and luminance contrast** *Vision Research* **107**:49–57

Kubilius J *et al.* (2019) **861 Brain-like object recognition with high-performing shallow recurrent ANNs** *Advances in neural information 862 processing systems* **32**

Kubilius J, Schrimpf M, Nayebi A, Bear D, Yamins DL, DiCarlo JJ (2018) **Cornet: Modeling the neural mechanisms of core object recognition** *BioRxiv*

Oram MW, Perrett DI (1994) **Modeling visual recognition from neurobiological constraints** *Neural Networks* **7**:945–972

Peyrin C, Michel CM, Schwartz S, Thut G, Seghier M, Landis T, Marendaz C, Vuilleumier P. (2010) **The neural substrates 868 and timing of top–down processes during coarse-to-fine categorization of visual scenes: A combined fMRI 869 and ERP study** *Journal of cognitive neuroscience* **22**:2768–2780

Purushothaman G, Chen X, Yampolsky D, Casagrande VA (2014) **Neural mechanisms of coarse-to-fine discrimination in the visual cortex** *Journal of Neurophysiology* **112**:2822–2833

Rokszin AA (2016) **Electrophysiological correlates of top-down effects facilitating natural image categorization are 873 disrupted by the attenuation of low spatial frequency information** *International journal of psychophysiology : offcial journal of the International Organization of Psychophysiology*

Rotshtein P, Schofield A, Funes MJ, Humphreys GW (2010) **Effects of spatial frequency bands on perceptual decision: It is not the stimuli but the comparison** *Journal of vision* **10**:25–25

Saneyoshi A, Michimata C. (2015) **Categorical and coordinate processing in object recognition depends on different spatial frequencies** *Cognitive Processing* **16**:27–33

Schyns PG, Oliva A. (1994) **From blobs to boundary edges: Evidence for time-and spatial-scale-dependent scene recognition** *Psychological science* **5**:195–200

Toosi R, Akhaee MA, Dehaqani MRA (2021) **An automatic spike sorting algorithm based on adaptive spike detection and a mixture of skew-t distributions** *Scientific Reports* **11**:1–18

Toosi R, Akhaee MA, Dehaqani MRA (2022) **Brain-inspired feedback for spatial frequency aware artificial networks** *In: 2022 56th Asilomar Conference on Signals, Systems, and Computers* :806–810

Yardley H, Perlovsky L, Bar M. (2012) **Predictions and incongruency in object recognition: A cognitive neuroscience perspective** *Detection and identification of rare audiovisual cues* :139–153

Zhang Y, Schriver KE, Hu JM, Roe AW (2023) **Spatial frequency representation in V2 and V4 of macaque monkey** *Elife* **12**

Editors

Reviewing Editor
Kristine Krug
Otto-von-Guericke University Magdeburg, Magdeburg, Germany

Senior Editor
Tirin Moore
Howard Hughes Medical Institute, Stanford University, Stanford, United States of America

Reviewer #1 (Public Review):

This study reports that spatial frequency representation can predict category coding in the inferior temporal cortex. The original conclusion was based on likely problematic stimulus timing (33 ms which was too brief). Now the authors claim that they also have a different set of data on the basis of longer stimulus duration (200 ms).

One big issue in the original report was that the experiments used a stimulus duration that was too brief and could have weakened the effects of high spatial frequencies and confounded the conclusions. Now the authors provided a new set of data on the basis of a longer stimulus duration and made the claim that the conclusions are unchanged. These new data and the data in the original report were collected at the same time as the authors report.

The authors may provide an explanation why they performed the same experiments using two stimulus durations and only reported one data set with the brief duration. They may also explain why they opted not to mention in the original report the existence of another data set with a different stimulus duration, which would otherwise have certainly strengthened their main conclusions.

I suggest the authors upload both data sets and analyzing codes, so that the claim could be easily examined by interested readers.

https://doi.org/10.7554/eLife.93589.2.sa1

Reviewer #2 (Public Review):

Summary:

This paper aimed to examine the spatial frequency selectivity of macaque inferotemporal (IT) neurons and its relation to category selectivity. The authors suggest in the present study that some IT neurons show a sensitivity for the spatial frequency of scrambled images. Their report suggests a shift in preferred spatial frequency during the response, from low to high spatial frequencies. This agrees with a coarse-to-fine processing strategy, which is in line with multiple studies in the early visual cortex. In addition, they report that the selectivity for faces and objects, relative to scrambled stimuli, depends on the spatial frequency tuning of the neurons.

Strengths:

Previous studies using human fMRI and psychophysics studied the contribution of different spatial frequency bands to object recognition, but as pointed out by the authors little is known about the spatial frequency selectivity of single IT neurons. This study addresses this gap and shows spatial frequency selectivity in IT for scrambled stimuli that drive the neurons poorly. They related this weak spatial frequency selectivity to category selectivity, but these findings are premature given the low number of stimuli they employed to assess category selectivity.

The authors revised their manuscript and provided some clarifications regarding their experimental design and data analysis. They responded to most of my comments but I find that some issues were not fully or poorly addressed. The new data they provided confirmed my concern about low responses to their scrambled stimuli. Thus, this paper shows spatial frequency selectivity in IT for scrambled stimuli that drive the neurons poorly (see main

comments below). They related this (weak) spatial frequency selectivity to category selectivity, but these findings are premature given the low number of stimuli to assess category selectivity.

Main points.

(1) They have provided now the responses of their neurons in spikes/s and present a distribution of the raw responses in a new Figure. These data suggest that their scrambled stimuli were driving the neurons rather poorly and thus it is unclear how well their findings will generalize to more effective stimuli. Indeed, the mean net firing rate to their scrambled stimuli was very low: about 3 spikes/s. How much can one conclude when the stimuli are driving the recorded neurons that poorly? Also, the new Figure 2- Appendix 1 shows that the mean modulation by spatial frequency is about 2 spikes/s, which is a rather small modulation. Thus, the spatial frequency selectivity the authors describe in this paper is rather small compared to the stimulus selectivity one typically observes in IT (stimulus-driven modulations can be at least 20 spikes/s).
(2) Their new Figure 2-Appendix 1 does not show net firing rates (baseline-subtracted; as I requested) and thus is not very informative. Please provide distributions of net responses so that the readers can evaluate the responses to the stimuli of the recorded neurons.
(3) The poor responses might be due to the short stimulus duration. The authors report now new data using a 200 ms duration which supported their classification and latency data obtained with their brief duration. It would be very informative if the authors could also provide the mean net responses for the 200 ms durations to their stimuli. Were these responses as low as those for the brief duration? If so, the concern of generalization to effective stimuli that drive IT neurons well remains.
(4) I still do not understand why the analyses of Figures 3 and 4 provide different outcomes on the relationship between spatial frequency and category selectivity. I believe they refer to this finding in the Discussion: "Our results show a direct relationship between the population's category coding capability and the SF coding capability of individual neurons. While we observed a relation between SF and category coding, we have found uncorrelated representations. Unlike category coding, SF relies more on sparse, individual neuron representations.". I believe more clarification is necessary regarding the analyses of Figures 3 and 4, and why they can show different outcomes.
(5) The authors found a higher separability for faces (versus scrambled patterns) for neurons preferring high spatial frequencies. This is consistent for the two monkeys but we are dealing here with a small amount of neurons. Only 6% of their neurons (16 neurons) belonged to this high spatial frequency group when pooling the two monkeys. Thus, although both monkeys show this effect I wonder how robust it is given the small number of neurons per monkey that belong to this spatial frequency profile. Furthermore, the higher separability for faces for the low-frequency profiles is not consistent across monkeys which should be pointed out.
(6) I agree that CNNs are useful models for ventral stream processing but that is not relevant to the point I was making before regarding the comparison of the classification scores between neurons and the model. Because the number of features and trial-to-trial variability differs between neural nets and neurons, the classification scores are difficult to compare. One can compare the trends but not the raw classification scores between CNN and neurons without equating these variables.

https://doi.org/10.7554/eLife.93589.2.sa0

Author response:

The following is the authors' response to the original reviews.

> ***Public Reviews:***
>
> ***Reviewer #1 (Public Review):***
>
> *Summary:*
>
> *This study reports that IT neurons have biased representations toward low spatial frequency*
>
> *(SF) and faster decoding of low SFs than high SFs. High SF-preferred neurons, and low SF-preferred neurons to a lesser degree, perform better category decoding than neurons with other profiles (U and inverted U shaped). SF coding also shows more sparseness than category coding in the earlier phase of the response and less sparseness in the later phase. The results are also contrasted with predictions of various DNN models.*
>
> *Strengths:*
>
> *The study addressed an important issue on the representations of SF information in a high-level visual area. Data are analyzed with LDA which can effectively reduce the dimensionality of neuronal responses and retain category information.*

We would like to express our sincere gratitude for your insightful and constructive comments which greatly contributed to the refinement of the manuscript. We appreciate the time and effort you dedicated to reviewing our work and providing suggestions. We have carefully considered each of your comments and addressed the suggested revisions accordingly.

> *Weaknesses:*
>
> *The results are likely compromised by improper stimulus timing and unmatched spatial frequency spectrums of stimuli in different categories.*
>
> *The authors used a very brief stimulus duration (35ms), which would degrade the visual system's contrast sensitivity to medium and high SF information disproportionately (see Nachmias, JOSAA, 1967). Therefore, IT neurons in the study could have received more degraded medium and high SF inputs compared to low SF inputs, which may be at least partially responsible for higher firing rates to low SF R1 stimuli (Figure 1c) and poorer recall performance with median and high SF R3-R5 stimuli in LDA decoding. The issue may also to some degree explain the delayed onset of recall to higher SF stimuli (Figure 2a), preferred low SF with an earlier T1 onset (Figure 2b), lower firing rate to high SF during T1 (Figure 2c), somewhat increased firing rate to high SF during T2 (because weaker high SF inputs would lead to later onset, Figure 2d).*

We appreciate your concern regarding the course-to-fine nature of SF processing in the vision hierarchy and the short exposure time of our paradigm. According to your comment, we repeated the analysis of SF representation with 200ms exposure time as illustrated in Appendix 1 - Figure 4. Our recorded data contains the 200ms version of exposure time for all neurons in the main phase. As can be seen, the results are similar to what we found with 33 ms experiments.

Next, we bring your attention to the following observations:

(1) According to Figure 2d, the average firing rate of IT neurons for HSF could be higher than LSF in the late response phase. Therefore, the amount of HSF input received by the IT neurons is as much as LSF, however, its impact on the IT response is observable in the later phase of the response. Thus, the LSF preference is because of the temporal advantage of the LSF processing rather than contrast sensitivity.

(2) According to Figure 3a, 6% of the neurons are HSF-preferred and their firing rate in HSF is comparable to the LSF firing rate in the LSF-preferred group. This analysis is carried out in the early phase of the response (70-170 ms). While most of the neurons prefer LSF, this observation shows that there is an HSF input that excites a small group of neurons. Furthermore, the highest separability index also belongs to the HSF-preferred profile in the early phase of the response which supports the impact of the HSF part of the input.

(3) Similar LSF-preferred responses are also reported by Chen et al. (2018) (50ms for SC) and Zhang et al. (2023) (3.5 - 4 secs for V2 and V4) for longer duration times.

Our results suggest that the LSF-preferred nature of the IT responses in terms of firing rate and recall, is not due to the weakness or lack of input source (or information) for HSF but rather to the processing nature of the SF in the vision hierarchy.

To address this issue in the manuscript:

Figure Appendix 1 - Figure 4 is added to the manuscript and shows the recall value and onset for R1-R5 with 200ms of exposure time.

We added the following description to the discussion:

“To rule out the degraded contrast sensitivity of the visual system to medium and high SF information because of the brief exposure time, we repeated the analysis with 200ms exposure time as illustrated in Appendix 1 - Figure 4 which indicates the same LSF-preferred results. Furthermore, according to Figure 2, the average firing rate of IT neurons for HSF could be higher than LSF in the late response phase. It indicates that the amount of HSF input received by the IT neurons in the later phase is as much as LSF, however, its impact on the IT response is observable in the later phase of the response. Thus, the LSF preference is because of the temporal advantage of the LSF processing rather than contrast sensitivity. Next, according to Figure 3(a), 6\% of the neurons are HSF-preferred and their firing rate in HSF is comparable to the LSF firing rate in the LSF-preferred group. This analysis is carried out in the early phase of the response (70-170ms). While most of the neurons prefer LSF, this observation shows that there is an HSF input that excites a small group of neurons. Additionally, the highest SI belongs to the HSF-preferred profile in the early phase of the response which supports the impact of the HSF part of the input. Similar LSF-preferred responses are also reported by Chen et. al. (2018) (50ms for SC) and Zhang et. al. (2023) (3.5 - 4 secs for V2 and V4). Therefore, our results show that the LSF-preferred nature of the IT responses in terms of firing rate and recall, is not due to the weakness or lack of input source (or information) for HSF but rather to the processing nature of the SF in the IT cortex.”

> *Figure 3b shows greater face coding than object coding by high SF and to a lesser degree by low SF neurons. Only the inverted-U-shaped neurons displayed slightly better object coding than face coding. Overall the results give an impression that IT neurons are significantly more capable of coding faces than coding objects, which is inconsistent with the general understanding of the functions of IT neurons. The problem may lie with the selection of stimulus images (Figure 1b). To study SF-related category coding, the images in two categories need to have similar SF spectrums in the Fourier domain. Such efforts are not mentioned in the manuscript, and a look at the images in Figure 1b suggests that such efforts are likely not properly made. The ResNet18 decoding results in Figure 6C, in that IT neurons of different profiles show similar face and object coding, might be closer to reality.*

Because of the limited number of stimuli in our experiments, it is hard to discuss the category selectivity, which needs a higher number of stimuli. To overcome the limited number of stimuli in our experiment, we fixed 60% (nine out of 15 stimuli) while varying the remaining

stimuli to reduce the selective bias. To check the coding capability of the IT neurons for face and non-face objects, we evaluated the recall of face vs. non-face classification in intact stimuli (similar to classifiers stated in the manuscript). Results show that at the population level, the recall value for objects is 90.45%, and for faces is 92.45%. However, the difference is not significant (p-value=0.44). On the other hand, we note that a large difference in the SI value does not translate directly to the classification accuracy, rather it illustrates the strength of representation.

Regarding the SF spectrums, after matching the luminance and contrast of the images we matched the power of the images concerning SF and category. Powers are calculated using the sum of the absolute value of the Fourier transform of the image. Considering all stimuli, the ANOVA analysis shows that various SF bands have similar power (one-way ANOVA, p-value=0.24). Furthermore, comparing the power of faces and images in all SF bands (including intact) and both unscrambled and scrambled images indicates no significant difference between face and object (p-vale > 0.1). Therefore, the result of Figure 3b suggests that IT employs various SF bands for the recognition of various objects.

Comparing the results of CNNs and IT shows that the CNNs do not capture the complexities of the IT cortex in terms of SF. One of the sources of this difference is because of the behavioral saliency of the face stimulus in the training of the primate visual system.

To address this issue in the manuscript:

The following description is added to the discussion:

"… the decoding performance of category classification (face vs. non-face) in intact stimuli is 94.2%. The recall value for objects vs. scrambled is 90.45%, and for faces vs. scrambled is 92.45% (p-value=0.44), which indicates the high level of generalizability and validity characterizing our results."

The following description is added to the method section, SF filtering.

"Finally, we equalized the stimulus power in all SF bands (intact, R-R5). The SF power among all conditions (all SF bands, face vs. non-face and unscrambled vs. scrambled) does not vary significantly (p-value > 0.1). SF power is calculated as the sum of the square value of the image coefficients in the Fourier domain."

> ***Reviewer #2 (Public Review):***
>
> *Summary:*
>
> *This paper aimed to examine the spatial frequency selectivity of macaque inferotemporal (IT) neurons and its relation to category selectivity. The authors suggest in the present study that some IT neurons show a sensitivity for the spatial frequency of scrambled images. Their report suggests a shift in preferred spatial frequency during the response, from low to high spatial frequencies. This agrees with a coarse-to-fine processing strategy, which is in line with multiple studies in the early visual cortex. In addition, they report that the selectivity for faces and objects, relative to scrambled stimuli, depends on the spatial frequency tuning of the neurons.*
>
> *Strengths:*
>
> *Previous studies using human fMRI and psychophysics studied the contribution of different spatial frequency bands to object recognition, but as pointed out by the authors little is known about the spatial frequency selectivity of single IT neurons. This study addresses this gap and they show that at least some IT neurons show a sensitivity for spatial frequency and*

> *interestingly show a tendency for coarse-to-fine processing.*

We extend our sincere appreciation for your thoughtful and constructive feedback on our paper. We are grateful for the time and expertise you invested in reviewing our work. Your detailed suggestions have been instrumental in addressing several key aspects of the paper, contributing to its clarity and scholarly merit. We have carefully considered each of your comments and have made revisions accordingly.

> *Weaknesses and requested clarifications:*
>
> *(1) It is unclear whether the effects described in this paper reflect a sensitivity to spatial frequency, i.e. in cycles/ deg (depends on the distance from the observer and changes when rescaling the image), or is a sensitivity to cycles /image, largely independent of image scale. How is it related to the well-documented size tolerance of IT neuron selectivity?*

Our stimuli are filtered using cycles/images and knowing the distance of the subject to the monitor, we can calculate the cycles/degrees. To the best of our knowledge, this is also the case for all other SF-related studies. To find the relation of observations to the cycles/image and degree/image, one should keep one of them fixed while changing the other, for example changing the subject's distance to the monitor will change the SF content in terms of cycle/degree. With our current data, we cannot discriminate this effect. To address this issue, we added the following description to the discussion. To address this issue, we added the following description to the discussion:

“Finally, since our experiment maintains a fixed SF content in terms of both cycles per degree and cycles per image, further experiments are needed to discern whether our observations reflect sensitivity to cycles per degree or cycles per image.”

> *(2) The authors' band-pass filtered phase scrambled images of faces and objects. The original images likely differed in their spatial frequency amplitude spectrum and thus it is unclear whether the differing bands contained the same power for the different scrambled images. If not, this could have contributed to the frequency sensitivity of the neurons.*

After equalizing the luminance and contrast of the images, we equilized their power concerning SF and category. The powers were calculated using the sum of the absolute values of the Fourier transform of the images. The results of the ANOVA analysis across all stimuli indicate that various SF bands exhibit similar power (one-way ANOVA, p-value = 0.24). Additionally, a comparison of power between faces and objects in all SF bands (including intact), for both unscrambled and scrambled images, reveals no significant differences (p-value > 0.1). To clarify this point, we have incorporated the following information into the Methods section.

“Finally, we equalized the stimulus power in all SF bands (intact, R-R5). The SF power among all conditions (all SF bands, face vs. non-face and unscrambled vs. scrambled) does not vary significantly (ANOVA, p-value > 0.1).”

> *(3) How strong were the responses to the phase-scrambled images? Phase-scrambled images are expected to be rather ineffective stimuli for IT neurons. How can one extrapolate the effect of the spatial frequency band observed for ineffective stimuli to that for more effective stimuli, like objects or (for some neurons) faces? A distribution should be provided, of the net responses (in spikes/s) to the scrambled stimuli, and this for the early and late windows.*

The sample neuron in Figure 1c is chosen to be a good indicator of the recorded neurons. In the early response phase, the average firing rate to scrambled stimuli is 26.3 spikes/s which is significantly higher than the response in -50 to 50ms which is 23.4. In comparison, the mean response to intact face stimuli is 30.5 spikes/s, while object stimuli elicit an average response of 28.8 spikes/s. Moving to the late phase, T2, the responses to scrambled, face, and object stimuli are 19.5, 19.4, and 22.4 spikes/s, respectively. Moreover, when the classification accuracy for SF exceeds chance levels, it indicates a significant impact of SF bands on the IT response. This raises a direct question about the explicit coding for SF bands in the IT cortex observed for ineffective stimuli and how it relates to complex and effective stimuli, such as faces. To show the strength of neuron responses to the SF bands in scrambled images, We added Appendix 1 - Figure 2 and also added Appendix 1 - Figure 1, according to comment 4, which shows the average and std of the responses to all SF bands. The following description is added to the results section.

“Considering the strength of responses to scrambled stimuli, the average firing rate in response to scrambled stimuli is 26.3 Hz, which is significantly higher than the response observed between -50 and 50 ms, where it is 23.4 Hz (p-value=3x10-5). In comparison, the mean response to intact face stimuli is 30.5 Hz, while non-face stimuli elicit an average response of 28.8 Hz. The distribution of neuron responses for scrambled, face, and non-face in T1 is illustrated in Appendix 1 - Figure 2.

[…]

Moreover, the average firing rates of scrambled, face, and non-face stimuli are 19.5 Hz, 19.4 Hz, and 22.4 Hz, respectively. The distribution of neuron responses is illustrated in Appendix 1 Figure 2.”

> *(4) The strength of the spatial frequency selectivity is unclear from the presented data. The authors provide the result of a classification analysis, but this is in normalized units so that the reader does not know the classification score in percent correct. Unnormalized data should be provided. Also, it would be informative to provide a summary plot of the spatial frequency selectivity in spikes/s, e.g. by ranking the spatial frequency bands for each neuron based on half of the trials and then plotting the average responses for the obtained ranks for the other half of the trials. Thus, the reader can appreciate the strength of the spatial frequency selectivity, considering trial-to-trial variability. Also, a plot should be provided of the mean response to the stimuli for the two analysis windows of Figure 2c and 2d in spikes/s so one can appreciate the mean response strengths and effect size (see above).*

The normalization of the classification result is just obtained by subtracting the chance level, which is 0.2, from the whole values. Therefore the values could still be interpreted in percent as we did in the results section. To make this clear, we removed the “a.u.” from the figure and we added the following description to the results section.

“The accuracy value is normalized by subtracting the chance level (0.2).”

Regarding the selectivity of the neuron, as suggested by your comment, we added a new figure in the appendix section, Appendix 1 - figure 2. This figure shows the strength of SF selectivity, considering trial-to-trial variability. The following description is added to the results section:

“The strength of SF selectivity, considering the trial-to-trial variability is provided in Appendix 1 Figure 2, by ranking the SF bands for each neuron based on half of the trials and then plotting the average responses for the obtained ranks for the other half of the trials.”

The firing rates of Figures 2c and 2d are normalized for better illustration since the variation in firing rates is high across neurons, as can be observed in Figure Appendix 1 - Figure 1. Since we seek trends in the response, the absolute values are not important (since the baseline firing rates of neurons are different), but the values relative to the baseline firing rate determine the trend. To address the mean response and the strength of the SF response, the following description is added to the results section.

“Considering the strength of responses to scrambled stimuli, the average firing rate in response to scrambled stimuli is 26.3 Hz, which is significantly higher than the response observed between -50 and 50 ms, where it is 23.4 Hz (p-value=3x10-5). In comparison, the mean response to intact face stimuli is 30.5 Hz, while non-face stimuli elicit an average response of 28.8 Hz. The distribution of neuron responses for scrambled, face, and non-face in T1 is illustrated in Appendix 1 - Figure 2.

[…]

Moreover, the average firing rates of scrambled, face, and non-face stimuli are 19.5 Hz, 19.4

Hz, and 22.4 Hz, respectively. The distribution of neuron responses is illustrated in Appendix 1 Figure 2.”

Furthermore, we added a figure, Appendix 1 - Figure 3, to illustrate the strength of SF selectivity in our profiles. The following is added to the results section:

“To check the robustness of the profiles, considering the trial-to-trial variability, the strength of SF selectivity in each profile is provided in Appendix 1 - Figure 3, by forming the profile of each neuron based on half of the trials and then plotting the average SF responses with the other

half of the trials.”

(5) It is unclear why such brief stimulus durations were employed. Will the results be similar, in particular the preference for low spatial frequencies, for longer stimulus durations that are more similar to those encountered during natural vision?

Please refer to the first comment of Reviewer 1.

> *(6) The authors report that the spatial frequency band classification accuracy for the population of neurons is not much higher than that of the best neuron (line 151). How does this relate to the SNC analysis, which appears to suggest that many neurons contribute to the spatial frequency selectivity of the population in a non-redundant fashion? Also, the outcome of the analyses should be provided (such as SNC and decoding (e.g. Figure 1D)) in the original units instead of undefined arbitrary units.*

The population accuracy is approximately 5% higher than the best neuron. However, we have no reference to compare the effect size (the value is roughly similar for face vs object while the chance levels are different). However, as stated in Methods, SNC is calculated for two label modes (LSF and HSF) and it can not be directly compared to the best neuron accuracy. Regarding the unit of SNC, it can be interpreted directly to percent by multiplying by a factor of 100. We removed the “a.u.” to prevent misunderstanding and modified the results section for clearance.

“… SNC score for SF (two labels, LSF (R1 and R2) vs. HSF (R4 and R5)) and category … (average SNC for SF=0.51\%±0.02 and category=0.1\%±0.04 …”

> *(7) To me, the results of the analyses of Figure 3c,d, and Figure 4 appear to disagree. The latter figure shows no correlation between category and spatial frequency classification accuracies while Figure 3c,d shows the opposite.*

In Figure 3c,d, following what we observed in Figure 3a,b about the category coding capabilities in the population of neurons based on the profile of the single neurons, we tested a similar idea if the coding capability of single neurons in SF/category could predict the coding capability of population neurons in terms of category/SF. Therefore, both analyses investigate a relation between a characteristic of single neurons and the coding capability of a population of similar neurons. On the other hand, in Figure 4, the idea is to check the characteristics of the coding mechanisms behind SF and category coding. In Figure 4a, we check if there exists any relation between category and SF coding capability within a single neuron activity without the impact of other neurons, to investigate the idea that SF coding may be a byproduct of an object recognition mechanism. In Figure 4b, we investigated the contribution of all neurons in population decision, again to check whether the mechanisms behind the SF and category coding are the same or not. This analysis shows how individual neurons contribute to SF or category coding at the population level. Therefore, the experiments in Figures 3 and 4 are different in the analysis method and what they were designed to investigate and we cannot directly compare the results.

> *(8) If I understand correctly, the "main" test included scrambled versions of each of the "responsive" images selected based on the preceding test. Each stimulus was presented 15 times (once in each of the 15 blocks). The LDA classifier was trained to predict the 5 spatial frequency band labels and they used 70% of the trials to train the classifier. Were the trained and tested trials stratified with respect to the different scrambled images? Also, LDA assumes a normal distribution. Was this the case, especially because of the mixture of repetitions of the same scrambled stimulus and different scrambled stimuli?*

In response to your inquiry regarding the stratification of trials, both the training and testing data were representative of the entire spectrum of scrambled images used in our experiment. To address your concern about the assumption of a normal distribution, especially given the mixture of repetitions of the same scrambled stimulus and different stimuli, our analysis of firing rates reveals a slightly left-skewed normal distribution. While there is a deviation from a perfectly normal distribution, we are confident that this skewness does not compromise the robustness of the LDA classifier.

> *(9) The LDA classifiers for spatial frequency band (5 labels) and category (2 labels) have different chance and performance levels. Was this taken into account when comparing the SNC between these two classifiers? Details and SNC values should be provided in the original (percent difference) instead of arbitrary units in Figure 5a. Without such details, the results are impossible to evaluate.*

For both SNC and CMI calculations in SF, we considered two labels of HSF (R4 and R5) and LSF (R1 and R2). This was mentioned in the Methods section, after equation (5). According to your comment, to make it clear in the results section, we also added this description to the results section.

"… illustrates the SNC score for SF (two labels, LSF (R1 and R2) vs. HSF (R4 and R5)) and category (face vs. non-face) … conditioned on the label, SF (LSF (R1 and R2) vs. HSF (R4 and R5)) or category, to assess the information."

The value of SNC can also be directly converted to the percent by a factor of 100. To make it clear, we removed "a.u." from the y-axis.

> *(10) Recording locations should be described in IT, since the latter is a large region. Did their recordings include the STS? A/P and M/L coordinate ranges of recorded neurons?*

We appreciate your suggestion for the recording location. Nevertheless, given the complexities associated with neurophysiological recordings and the limitations imposed by our methodologies, we face challenges in precisely localizing every unit if they are located in STS or not. To address your comment, We added Appendix 1 - Figure 5 which shows the SF and category coding capability of neurons along their recorded locations.

> *(11) The authors should show in Supplementary Figures the main data for each of the two animals, to ensure the reader that both monkeys showed similar trends.*

We added Appendix 2 which shows the consistency of the main results in the two monkeys.

> *(12) The authors found that the deep nets encoded better the spatial frequency bands than the IT units. However, IT units have trial-to-trial response variability and CNN units do not. Did they consider this when comparing IT and CNN classification performance? Also, the number of features differs between IT and CNN units. To me, comparing IT and CNN classification performances is like comparing apples and oranges.*

Deep convolutional neural networks are currently considered the state-of-the-art models of the primate visual pathway. However, as you mentioned and based on our results, they do not yet capture various complexities of the visual ventral stream. Yet studying the similarities and differences between CNN and brain regions, such as the IT cortex, is an active area of research, such as:

a. Kubilius, Jonas, et al. "Brain-like object recognition with high-performing shallow recurrent ANNs." Advances in neural information processing systems 32 (2019).

b. Xu, Yaoda, and Maryam Vaziri-Pashkam. "Limits to visual representational correspondence between convolutional neural networks and the human brain." Nature Communications, 12.1 (2021).

c. Jacob, Georgin, et al. "Qualitative similarities and differences in visual object representations between brains and deep networks." Nature Communications, 12.1 (2021).

Therefore, we believe comparing IT and CNN, despite all of the differences in terms of their characteristics, can help both fields grow faster, especially in introducing brain-inspired networks.

> *(13) The authors should define the separability index in their paper. Since it is the main index to show a relationship between category and spatial frequency tuning, it should be described in detail. Also, results should be provided in the original units instead of undefined arbitrary units. The tuning profiles in Figure 3A should be in spikes/s. Also, it was unclear to me whether the classification of the neurons into the different tuning profiles was based on an ANOVA assessing per neuron whether the effect of the spatial frequency band was significant (as should be done).*

Based on your comment, we added the description of the separability index to the methods section. However, since the separability index is defined as the division of two dispersion matrices, it has no units by nature. The tuning profiles in Figure 3a are normalized for better illustration since the variation in firing rates is high. Since we seek trends in the response, the absolute values are not important. Regarding the SF profile formation, to better present the

SF profile assignment, we updated the method section. Furthermore, The strength of responses for scrambled stimuli can be observed in Appendix 1 - Figures 1 and 2.

> *(14) As mentioned above, the separability analysis is the main one suggesting an association between category and spatial frequency tuning. However, they compute the separability of each category with respect to the scrambled images. Since faces are a rather homogeneous category I expect that IT neurons have on average a higher separability index for faces than for the more heterogeneous category of objects, at least for neurons responsive to faces and/or objects. The higher separability for faces of the two low- and high-pass spatial frequency neurons could reflect stronger overall responses for these two classes of neurons. Was this the case? This is a critical analysis since it is essential to assess whether it is category versus responsiveness that is associated with the spatial frequency tuning. Also, I do not believe that one can make a strong claim about category selectivity when only 6 faces and 3 objects (and 6 other, variable stimuli; 15 stimuli in total) are employed to assess the responses for these categories (see next main comment). This and the above control analysis can affect the main conclusion and title of the paper.*

We appreciate your concern regarding category selectivity or responsiveness of the SF profiles. First, we note that we used SI since it overcomes the limitations of the accuracy and recall metrics as they are discrete and can be saturated. Using SI, we cannot directly calculate face vs object with SI, since this index only reports one value for the whole discrimination task. Therefore, we have to calculate the SI for face/object vs scrambled to obtain a value per category. However, as you suggested, it raises the question of whether we assess how well the neural responses distinguish between actual images (faces or objects) and their scrambled versions or if we just assess the responsiveness. Based on Figure 3b, since we have face-selective (LSF and HSF preferred profiles), object-selective (inverse U), and the U profile, where SI is the same for both face and object, we believe the SF profile is associated with the category selectivity, otherwise we would have the same face/object recall in all profiles, as we have in the U shape profile.

To analyze this issue further, we calculated the number of face/object selective neurons in 70-170ms. We found 43 face-selective neurons and 36 object-selective neurons (FDR corrected p-value < 0.05). Therefore, the number of face-selective and object-selective neurons is similar. Next, we check the selectivity of the neurons within each profile. Number of face/object selective neurons is LP=13/3, HP=6/2, IU=3/9, U=14/13, and the remaining belong to the NP group. Results show higher face-selective neurons in LP and HP and a higher number of object-selective neurons in the IU class. The U class contains roughly the same number of face and object-selective neurons. This observation supports the relationship between category selectivity and profiles.

Next, we examined the average neuron response to the face and object in each profile. The difference between the firing rate of the face and object in none of the profiles was significant (Ranksum with a significance level of 0.05). However, the rates are as follows. The average firing rate (spikes/s) of face/object is LP=36.72/28.77, HP=28.55/25.52, IU=21.55/27.25, U=38.48/36.28. While the differences are not significant, they support the relationship between profiles and categories instead of responsiveness.

The following description is added to the results section to cover this point of view.

“To assess whether the SF profiles distinguish category selectivity or merely evaluate the neuron's responsiveness, we quantified the number of face/non-face selective neurons in the 70-170ms time window. Our analysis shows a total of 43 face-selective neurons and 36 non-face-selective neurons (FDR-corrected p-value < 0.05). The results indicate a higher proportion of face-selective neurons in LP and HP, while a greater number of non-face-

selective neurons is observed in the IU category (number of face/non-face selective neurons: LP=13/3, HP=6/2, IU=3/9). The U category exhibits a roughly equal distribution of face and non-face-selective neurons (U=14/13). This finding reinforces the connection between category selectivity and the identified profiles. We then analyzed the average neuron response to faces and non-faces within each profile. The difference between the firing rates for faces and non-faces in none of the profiles is significant (face/non-face average firing rate (Hz): LP=36.72/28.77, HP=28.55/25.52, IU=21.55/27.25, U=38.48/36.28, Ranksum with significance level of 0.05). Although the observed differences are not statistically significant, they provide support for the association between profiles and categories rather than mere responsiveness."

About the low number of stimuli, please check the next comment.

> *(15) For the category decoding, the authors employed intact, unscrambled stimuli. Were these from the main test? If yes, then I am concerned that this represents a too small number of stimuli to assess category selectivity. Only 9 fixed + 6 variable stimuli = 15 were in the main test. How many faces/ objects on average? Was the number of stimuli per category equated for the classification? When possible use the data of the preceding selectivity test which has many more stimuli to compute the category selectivity.*

We used only the main phase recorded data, which contains 15 images in each session. Each image results in 12 stimuli (intact, R1-R5, and phase-scrambled version). Thus, there exists a total of 180 unique stimuli in each session. Increasing the number of images would have increased the recording time. We compensated for this limitation by increasing the diversity of images in each session by picking the most responsive ones from the selectivity phase. On average, 7.54 of the stimuli were face in each session. We added this information to the Methods section. Furthermore, as mentioned in the discussion, for each classification run, the number of samples per category is equalized. We note that we cannot use the selectivity data for analysis, since the SF-related stimuli are filtered in different bands.

> ***Recommendations For The Authors:***
>
> ***Reviewer #1 (Recommendations For The Authors):***
>
> *I suggest that the authors double-check their results by performing control experiments with longer stimulus duration and SF-spectrum-matched face and object stimuli.*

Thanks for your suggestion, according to your comment, we added Appendix 1 - Figure 3.

> *In addition, I had a very difficult time understanding the differences between Figure 3c and Figure 4a. Please rewrite the descriptions to clarify.*

Thanks for your suggestion, we tried to revise the description of these two figures. The following description is added to the results section for Figure 3c.

"Next, to examine the relation between the SF (category) coding capacity of the single neurons and the category (SF) coding capability of the population level, we calculated the correlation between coding performance at the population level and the coding performance of single neurons within that population (Figure 3 c and d). In other words, we investigated the relation between single and population levels of coding capabilities between SF and category. The SF (or category) coding performance of a sub-population of 20 neurons that have roughly the same single-level coding capability of the category (or SF) is examined."

> *Lines 147-148: The text states that 'The maximum accuracy of a single neuron was 19.08% higher than the chance level'. However, in Figure 4, the decoding accuracies of*

> *individual neurons for category and SF range were between 49%-90% and 20%-40%, respectively.*
>
> *Please explain the discrepancies.*

The first number is reported according to chance level which is 20%, thus the unnormalized number is 39% which is consistent with the SF accuracy in Figure 4. We added the following description to prevent any misunderstanding.

"… was 19.08\% higher than the chance level (unnormalized accuracy is 49.08\%, neuron \#193, M2)."

> *Lines 264-265: Should 'the alternative for R3 and R4' be 'the alternative for R4 and R5'?*

Thanks for your attention, it's "R4 and R5". We corrected that mistake.

> *Lines 551-562: The labels for SF classification are R1-R5. Is it a binary or a multi-classification task?*

It's a multi-label classification. We made it clear in the text.

"… labels were SF bands (R1, R2, ..., R5, multi-label classifier)."

> *Figure 4b: Neurons in SF/category decoding exhibit both positive and negative weights. However, in the analysis of sparse neuron weights in Equation 6, only the magnitude of the weights is considered. Is the sign of weight considered too?*

We used the absolute value of the neuron weight to calculate sparseness. We also corrected Equation 6.

> ***Reviewer #2 (Recommendations For The Authors):***
>
> *(1) Line 52: what do the authors mean by coordinate processing in object recognition?*

To avoid any potential misunderstanding, we used the exact phrase in Saneyoshi and Michimata (2015). It is in fact, coordinate relations processing. Coordinate relations specify the metric information of the relative locations of objects.

> *(2) About half of the Introduction is a summary of the Results. This can be shortened.*

Thanks for your suggestion.

> *(3) Line 134: Peristimulus time histogram instead of Prestimulus time histogram.*

Thanks for your attention. We corrected that.

> *(4) Line 162: the authors state that R1 is decoded faster than R5, but the reported statistic is only for R1 versus R2.*

It was a typo, the p-value is only reported for R1 and R5.

> *(5) Line 576: which test was used for the asses the statistical significance?*

The test is Wilcoxon signed-rank. We added it to the text.

> *(6) How can one present a 35 ms long stimulus with a 60 Hz frame rate (the stimuli were presented on a 60Hz monitor (line 470))? Please correct.*

Thanks for your attention. We corrected that. The time of stimulus presentation is 33ms and the monitor rate is 120Hz.

https://doi.org/10.7554/eLife.93589.2.sa3